



COUPLED WAVES ON A PERIODICALLY SUPPORTED TIMOSHENKO BEAM

MARIA A. HECKL

Department of Mathematics, Keele University, Staffordshire ST5 5BG, England.

E-mail: m.a.heckl@maths.keele.ac.uk

(Received 26 September 2000, and in final form 6 June 2001)

A mathematical model is presented for the propagation of structural waves on an infinitely long, periodically supported Timoshenko beam. The wave types that can exist on the beam are bending waves with displacements in the horizontal and vertical directions, compressional waves and torsional waves. These waves are affected by the periodic supports in two ways: their dispersion relation spectra show passing and stopping bands, and coupling of the different wave types tends to occur. The model in this paper could represent a railway track where the beam represents the rail and an appropriately chosen support type represents the pad/sleeper/ballast system of a railway track. Hamilton's principle is used to calculate the Green function matrix of the free Timoshenko beam without supports. The supports are incorporated into the model by combining the Green function matrix with the superposition principle. Bloch's theorem is applied to describe the periodicity of the supports. This leads to polynomials with several solutions for the Bloch wave number. These solutions are obtained numerically for different combinations of wave types. Two support types are examined in detail: mass supports and spring supports. More complex support types, such as mass/spring systems, can be incorporated easily into the model.

© 2002 Elsevier Science Ltd. All rights reserved.

1. INTRODUCTION

This paper presents a mathematical model for the propagation of structural waves on an infinitely long, periodically supported Timoshenko beam. Several wave types can exist on the beam. These are bending waves with displacements in the horizontal and vertical direction, compressional waves and torsional waves. The waves are assumed to be harmonic with the same frequency. On a free beam without supports, these waves would propagate independently of each other with wavelengths depending on the geometry and material of the beam. On a periodically supported beam, which forms a periodic system, new effects occur: (1) the supports inflict a passing/stopping band (also called attenuation/propagation zone) behaviour on the waves; (2) the supports tend to couple different wave types if more than one wave type is present.

A Timoshenko beam is used in the model, rather than an Euler–Bernoulli beam. Timoshenko theory is more comprehensive than the Euler–Bernoulli theory in that the effects of shear deformation and rotary inertia, which affect bending waves, are included. It thus has the advantage of extending the validity of the model to a higher frequency range than would be the case with the Euler–Bernoulli theory.

The model presented in this paper offers a choice of different support types. A beam with mass supports, and a beam with spring supports are considered in detail. Supports in the form of mass/spring systems can easily be incorporated.

A real engineering structure, which could be represented by a periodically supported Timoshenko beam, is a railway track. The beam represents the rail, and this model would be valid at low and medium frequencies where cross-sectional deformation of the rail does not occur. At each support point, the beam is connected to a spring/mass/spring system, where the upper spring represents a rail pad, the mass represents a sleeper, and the lower spring, which rests on a rigid surface, represents the ballast bedded on compacted ground with a smooth surface.

A number of other authors have produced models of rail vibrations [1–4], which are limited to vertical bending waves. Munjal and Heckl [1] modelled the rail as an Euler beam on periodic mass supports and analyzed the propagation of vertical bending waves with a transfer matrix method. Kurze [2] compared various aspects of rail models, in particular, discrete supports versus a continuous rail support (Winkler foundation), and an Euler–Bernoulli beam versus a Timoshenko beam. In Nordborg’s work [3], the rail is modelled as an Euler beam, supported on flexible sleepers that can perform bending motion. Hamet [4] extended Nordborg’s work in that he used Timoshenko theory instead of Euler–Bernoulli theory for the rail; however, he did not include flexible sleepers in his model, but modelled the sleepers simply as rigid masses.

The behaviour of coupled waves on a periodically supported rail has received only limited attention so far. Coupled bending-compressional wave motion is analyzed in reference [5] for an Euler beam with spring-mounted masses. In a forerunner of the present paper, Heckl [6] studied the coupling of vertical bending waves, horizontal bending waves and torsional waves, but not compressional waves, on a periodically supported Timoshenko beam.

Mead’s studies [7–10] of wave propagation on more general periodic engineering structures have provided valuable insight into multiple coupling of waves. An extensive literature review on the subject can be found in reference [7]. Mead [8] predicted the number of free wave types that can propagate along a periodic structure. The bounding frequencies of passing and stopping bands are calculated in reference [9]. The propagation of vertical bending waves along a periodic Timoshenko beam is analyzed in reference [10].

The studies by Mace [11, 12] of the bending vibration of infinite fluid-loaded plates with periodic line supports are also of interest. Mace’s mathematical approach contains some elements that are also used in this paper, such as Fourier transforms and Bloch’s theorem (also called Floquet’s principle). The mathematical approach of Nordborg [3], Hamet [4] and Mead [10] is similar to that used here in that Green functions, the superposition principle and Bloch’s theorem are used.

Their studies are extended in the present paper by allowing beam deformations in all three spatial directions, not just in the vertical direction. Instead of the Green function, there is a Green function matrix. This is a 3×3 matrix with elements that are given by the responses in the x , y and z directions (lateral, vertical and axial direction) to unit point forces in the x , y and z directions. The elements of the Green function matrix are calculated in section 2 using Hamilton’s principle. This section is taken from a report by Heckl [13], which is repeated here, to make it available in the open literature.

In section 3, the beam supports are built into the mathematical model. This is done by combining the Green function matrix with the superposition principle. Free waves on the periodically supported beam are then studied by application of Bloch’s theorem. Different combinations of wave types will be examined. Numerical results are presented in section 4 in the form of spectra of the Bloch wave number (also called the propagation constant). The focus is on a beam with mass supports and one with spring supports. The behaviour for other support types is discussed briefly.

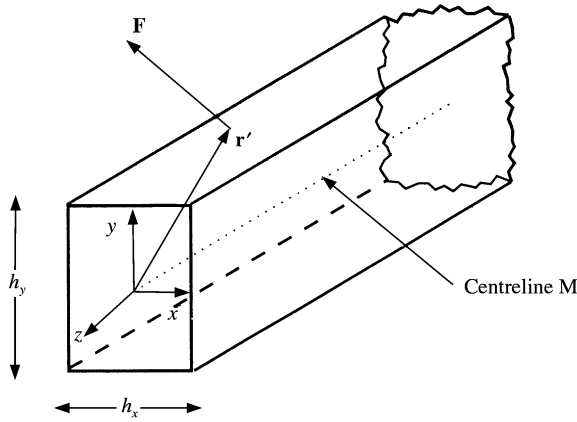


Figure 1. Geometry of the Timoshenko beam.

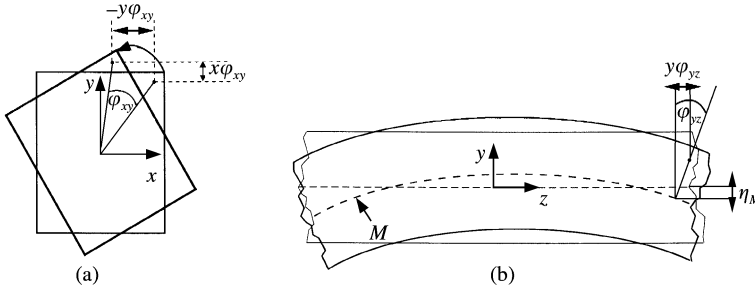


Figure 2. Notation for the different wave types on the beam: (a) cross-sectional rotation due to a torsional wave; (b) bending deformation in the y direction.

2. CALCULATION OF THE GREEN FUNCTION MATRIX OF THE UNSUPPORTED TIMOSHENKO BEAM

2.1. GENERAL CONSIDERATIONS

A uniform, infinitely long, Timoshenko beam is considered, with width h_x and height h_y (see Figure 1). A force vector \mathbf{F} with components (F_x, F_y, F_z) acts at a point $\mathbf{r}' = (x', y', z')$. The observer point is denoted by $\mathbf{r} = (x, y, z)$, and the displacement at this observer point is denoted by a vector with a lateral, vertical and axial component (ξ, η, ζ) .

The components of the displacement vector are given by

$$\xi(x, y, z) = \xi_M(z) - y\varphi_{xy}(z), \quad \eta(x, y, z) = \eta_M(z) + x\varphi_{xy}(z), \quad (2.1a, b)$$

$$\zeta(x, y, z) = \zeta_M(z) + x\varphi_{xz}(z) + y\varphi_{yz}(z). \quad (2.1c)$$

ξ_M, η_M and ζ_M are the displacements of the centreline M (see Figure 1) of the beam. φ_{xy} is the angle of torsion (see Figure 2(a)), φ_{xz} and φ_{yz} are the angles of rotation about the x - and y -axis respectively (see Figure 2(b)). These angles of rotation are partly due to bending and partly due to transverse shear deformation. The three centreline displacements and three angles form a set of six independent field quantities, which fully describe the motion of the beam.

The Green function here is a 3×3 matrix, which relates the force vector \mathbf{F} to the resulting displacements,

$$\begin{bmatrix} \zeta \\ \eta \\ \zeta \end{bmatrix} = \begin{bmatrix} G_{xx} & G_{xy} & G_{xz} \\ G_{yx} & G_{yy} & G_{yz} \\ G_{zx} & G_{zy} & G_{zz} \end{bmatrix} \begin{bmatrix} F_x \\ F_y \\ F_z \end{bmatrix}. \tag{2.2}$$

The elements of this Green function matrix are functions of \mathbf{r} and \mathbf{r}' , e.g., $G_{xx}(\mathbf{r}; \mathbf{r}')$. Their calculation will be done in two steps. In a first step (see section 2.2), a force distribution along a line parallel to the z -axis is considered. Hamilton’s principle will be applied to calculate the response of the beam to this loading. In a second step (see section 2.3), a point force is considered and the Fourier transform method will be applied to calculate the response of the beam to this point force. The time dependence is harmonic, described by the factor $e^{-i\omega t}$, which will be dropped throughout.

2.2. BEAM RESPONSE TO A SINUSOIDALLY DISTRIBUTED LOADING

The loading has vector components $F_{x'}$, $F_{y'}$, $F_{z'}$; they all have the z -dependence $e^{ik_z(z-z')}$ and can be written as

$$F_{x'} = F_x e^{ik_z(z-z')}, \quad F_{y'} = F_y e^{ik_z(z-z')}, \quad F_{z'} = F_z e^{ik_z(z-z')}. \tag{2.3a-c}$$

F_x, F_y, F_z are the force amplitudes. The same z -dependence is imposed on the displacements and angles, which can thus be written as

$$\zeta_M = A_1 e^{ik_z(z-z')} \quad (\text{bending displacement in the } x \text{ direction}), \tag{2.4a}$$

$$\eta_M = A_2 e^{ik_z(z-z')} \quad (\text{bending displacement in the } y \text{ direction}), \tag{2.4b}$$

$$\zeta_M = A_3 e^{ik_z(z-z')} \quad (\text{compressional displacement}), \tag{2.4c}$$

$$\varphi_{xy} = A_4 e^{ik_z(z-z')} \quad (\text{torsion}), \tag{2.4d}$$

$$\varphi_{xz} = A_5 e^{ik_z(z-z')} \quad (\text{bending and transverse shear in the } x \text{ direction}), \tag{2.4e}$$

$$\varphi_{yz} = A_6 e^{ik_z(z-z')} \quad (\text{bending and transverse shear in the } y \text{ direction}). \tag{2.4f}$$

$A_1 - A_6$ are complex amplitudes, which are unknown at this stage and will be determined with Hamilton’s principle.

Hamilton’s principle states that the motion of a mechanical system is such that the time integral

$$\Phi = \int (E_{kin} - E_{pot} + W_{ext}) dt \quad \text{is a minimum,} \tag{2.5}$$

where E_{kin} is the kinetic energy of the system, E_{pot} is its potential energy and W_{ext} is the external work applied to the system (see references [14, chapter 3.2], or [15, p. 157]).

This principle will be applied to the Timoshenko beam. First (see section 2.2.1), the Hamilton integral in equation (2.5) is expressed in terms of the field quantities and subsequently in terms of the unknown amplitudes. Then (see section 2.2.2), the Hamilton integral is minimized with respect to these amplitudes and a set of equations is obtained, which determines them fully.

2.2.1. Calculation of the Hamilton integral

The analysis will be simplified by two assumptions: the shear stress distribution remains uniform across the cross-section when a bending wave propagates along the beam; the cross-section does not warp when a torsional wave propagates along the beam.

In effect, the Timoshenko correction factor for the shear stiffness (first assumption) and the correction factor for the torsional stiffness (second assumption) are set equal to unity. Both correction factors depend on the cross-sectional shape, and the above assumptions are unlikely to make any qualitative difference to the numerical results for the rectangular beam considered in section 4.

2.2.1.1. Kinetic energy. The kinetic energy of the beam is expressed as a volume integral of the kinetic energy density,

$$E_{kin} = \frac{\rho}{2} \iiint (\dot{\xi}^2 + \dot{\eta}^2 + \dot{\zeta}^2) dx dy dz. \tag{2.6}$$

The time integral over E_{kin} , which, for harmonic time dependence, is equivalent to the time average $\overline{E_{kin}}$, is required for equation (2.5). It can easily be shown that time averages over the product of two harmonic field quantities, say $f_1(t) = \hat{f}_1 e^{-i\omega t}$ and $f_2(t) = \hat{f}_2 e^{-i\omega t}$, can be written in terms of their complex amplitudes \hat{f}_1 and \hat{f}_2 ,

$$\int f_1(t) f_2(t) dt = \frac{1}{2} \text{Re}(\hat{f}_1 \hat{f}_2^*), \tag{2.7}$$

where the * denotes the complex conjugate. With this result, one obtains

$$\overline{E_{kin}} = \frac{\rho}{4} \iiint (|\dot{\xi}|^2 + |\dot{\eta}|^2 + |\dot{\zeta}|^2) dx dy dz; \tag{2.8}$$

the \wedge which should denote the complex amplitudes has been dropped.

The time derivatives can be written with equation (2.1) as

$$|\dot{\xi}|^2 = \omega^2 |\zeta_M - y\varphi_{xy}|^2, \quad |\dot{\eta}|^2 = \omega^2 |\eta_M + x\varphi_{xy}|^2, \tag{2.9a, b}$$

$$|\dot{\zeta}|^2 = \omega^2 |\zeta_M + x\varphi_{xz} + y\varphi_{yz}|^2. \tag{2.9c}$$

2.2.1.2. Potential energy. The average potential energy is also calculated from the corresponding energy density and the use of complex amplitudes,

$$\overline{E_{pot}} = \frac{1}{4} \iiint (\sigma_z \varepsilon_z^* + \tau_{xy} \gamma_{xy}^* + \tau_{xz} \gamma_{xz}^* + \tau_{yz} \gamma_{yz}^*) dx dy dz. \tag{2.10}$$

σ_z and ε_z are the longitudinal stress and longitudinal strain respectively. ε_z is given by

$$\varepsilon_z = \frac{\partial \zeta}{\partial z} = ik_z (\zeta_M + x\varphi_{xz} + y\varphi_{yz}), \tag{2.11a}$$

where equation (2.1c) and the assumption of the z -dependence $e^{ik_z(z-z')}$ has been used. The corresponding strain is given by Hooke's law,

$$\sigma_z = E\varepsilon_z. \tag{2.11b}$$

E is the Young's modulus. Similarly, the shear strains γ and shear stresses τ are given by

$$\gamma_{xy} = \frac{\partial \xi}{\partial y} + \frac{\partial \eta}{\partial x} = 0, \quad \tau_{xy} = G\gamma_{xy} = 0, \tag{2.12a, b}$$

$$\gamma_{xz} = \frac{\partial \xi}{\partial z} + \frac{\partial \zeta}{\partial x} = ik_z(\xi_M - y\varphi_{xy}) + \varphi_{xz}, \quad \tau_{xz} = G\gamma_{xz}, \tag{2.13a, b}$$

$$\gamma_{yz} = \frac{\partial \eta}{\partial z} + \frac{\partial \zeta}{\partial y} = ik_z(\eta_M + x\varphi_{xy}) + \varphi_{yz}, \quad \tau_{yz} = G\gamma_{yz}. \tag{2.14a, b}$$

G is the shear modulus; it is related to the Young's modulus E by

$$G = E/2(1 + \mu), \tag{2.15}$$

where μ is the Poisson ratio.

2.2.1.3. *External work.* The line force with components $F_{x'}$, $F_{y'}$, $F_{z'}$ acts on the beam along a line parallel to the z -axis at position x' , y' . It supplies the external work

$$\overline{W_{ext}} = \frac{1}{2} \operatorname{Re} \iiint (F_{x'}\xi^* + F_{y'}\eta^* + F_{z'}\zeta^*) \delta(x - x') \delta(y - y') dx dy dz. \tag{2.16}$$

2.2.1.4. *Complete Hamilton integral.* With equations (2.8)–(2.14) and (2.16) (after integration with respect to x and y), the Hamilton integral Φ in equation (2.5) can be written as

$$\begin{aligned} \Phi &= \frac{1}{4} \omega^2 \rho \iiint \{ |\xi_M - y\varphi_{xy}|^2 + |\eta_M + x\varphi_{xy}|^2 + |\zeta_M + x\varphi_{xz} + y\varphi_{yz}|^2 \} dx dy dz \\ &\quad - \frac{1}{4} \iiint \{ Ek_z^2 |\zeta_M + x\varphi_{xz} + y\varphi_{yz}|^2 \\ &\quad + G |ik_z(\xi_M - y\varphi_{xy}) + \varphi_{xz}|^2 + G |ik_z(\eta_M + x\varphi_{xy}) + \varphi_{yz}|^2 \} dx dy dz \\ &\quad + \frac{1}{2} \operatorname{Re} \int \{ F_{x'}(z)\xi^*(x', y', z) + F_{y'}(z)\eta^*(x', y', z) + F_{z'}(z)\zeta^*(x', y', z) \} dz. \end{aligned} \tag{2.17}$$

The integrals over x and y span the cross-sectional area of the beam; only constant, linear and quadratic terms in x and y occur in the integrand. With

$$\int_{-h_x/2}^{h_x/2} \int_{-h_y/2}^{h_y/2} dx dy = h_x h_y, \tag{2.18a}$$

$$\int_{-h_x/2}^{h_x/2} \int_{-h_y/2}^{h_y/2} x dx dy = 0, \quad \int_{-h_x/2}^{h_x/2} \int_{-h_y/2}^{h_y/2} y dx dy = 0, \tag{2.18b, c}$$

$$\int_{-h_x/2}^{h_x/2} \int_{-h_y/2}^{h_y/2} x^2 dx dy = \frac{h_x^3 h_y}{12}, \quad \int_{-h_x/2}^{h_x/2} \int_{-h_y/2}^{h_y/2} y^2 dx dy = \frac{h_x h_y^3}{12}, \tag{2.18d, e}$$

one can perform the integration over x and y in the triple integrals of (2.17) and write Φ as

$$\begin{aligned} \Phi = & \frac{1}{4} \omega^2 \rho h_x h_y \int \left\{ |\zeta_M|^2 + \frac{h_y^2}{12} |\varphi_{xy}|^2 + |\eta_M|^2 + \frac{h_x^2}{12} |\varphi_{xy}|^2 + |\zeta_M|^2 + \frac{h_x^2}{12} |\varphi_{xz}|^2 + \frac{h_y^2}{12} |\varphi_{yz}|^2 \right\} dz \\ & - \frac{1}{4} h_x h_y \int \left\{ Ek_z^2 \left(|\zeta_M|^2 + \frac{h_x^2}{12} |\varphi_{xz}|^2 + \frac{h_y^2}{12} |\varphi_{yz}|^2 \right) \right. \\ & + G \left[k_z^2 |\zeta_M|^2 + k_z^2 \frac{h_y^2}{12} |\varphi_{xy}|^2 + |\varphi_{xz}|^2 + (ik_z \zeta_M \varphi_{xz}^* - ik_z \zeta_M^* \varphi_{xz}) \right] \\ & + G \left[k_z^2 |\eta_M|^2 + k_z^2 \frac{h_x^2}{12} |\varphi_{xy}|^2 + |\varphi_{yz}|^2 + (ik_z \eta_M \varphi_{yz}^* - ik_z \eta_M^* \varphi_{yz}) \right] \left. \right\} dz \\ & + \frac{1}{2} \text{Re} \int \left\{ F_{x'} (\zeta_M^* - y' \varphi_{xy}^*) + F_{y'} (\eta_M^* + x' \varphi_{xy}^*) + F_{z'} (\zeta_M^* + x' \varphi_{xz}^* + y' \varphi_{yz}^*) \right\} dz. \quad (2.19) \end{aligned}$$

The single integral in equation (2.17) has been rewritten with use of equations (2.1a-c).

Next, Φ will be expressed in terms of the amplitudes A_1 - A_6 and F_x, F_y, F_z by substituting equations (2.3a-c) and (2.4a-f) into equation (2.19). Any z -dependence in the integrand of (2.19) cancels out, so the integration over z can be ignored, and one obtains

$$\begin{aligned} \Phi = & \frac{1}{4} \omega^2 \rho h_x h_y \left\{ |A_1|^2 + |A_2|^2 + |A_3|^2 + \frac{h_x^2}{12} (|A_4|^2 + |A_5|^2) + \frac{h_y^2}{12} (|A_4|^2 + |A_6|^2) \right\} \\ & - \frac{1}{4} h_x h_y Ek_z^2 \left\{ |A_3|^2 + \frac{h_x^2}{12} |A_5|^2 + \frac{h_y^2}{12} |A_6|^2 \right\} \\ & - \frac{1}{4} h_x h_y G \left\{ k_z^2 (|A_1|^2 + |A_2|^2) + k_z^2 \left(\frac{h_x^2}{12} + \frac{h_y^2}{12} \right) |A_4|^2 + |A_5|^2 + |A_6|^2 \right. \\ & + ik_z (A_1 A_5^* - A_1^* A_5) + ik_z (A_2 A_6^* - A_2^* A_6) \left. \right\} \\ & + \frac{1}{4} \left\{ F_x (A_1^* - y' A_4^*) + F_x^* (A_1 - y' A_4) \right. \\ & + F_y (A_2^* + x' A_4^*) + F_y^* (A_2 + x' A_4) \\ & + F_z (A_3^* + x' A_5^* + y' A_6^*) + F_z^* (A_3 + x' A_5 + y' A_6) \left. \right\}. \quad (2.20) \end{aligned}$$

2.2.2. Minimization of the Hamilton integral

The Hamilton integral Φ is a quadratic function of the amplitudes A_1 - A_6 and has a unique minimum. This minimum can be found by setting the derivatives of Φ with respect to A_1 - A_6 equal to zero. The amplitudes are generally complex, so the differentiation has to be performed with respect to both the real and imaginary parts of these amplitudes for the minimization process. The following notation is used:

$$\frac{\partial}{\partial A_1} = \frac{\partial}{\partial (\text{Re } A_1)} + i \frac{\partial}{\partial (\text{Im } A_1)}, \text{ etc.} \quad (2.21)$$

The following relationships are valid, which simplify the differentiation considerably:

$$\frac{\partial |A_1|^2}{\partial A_1} = 2A_1, \text{ etc.}, \quad \frac{\partial (A_1 A_5^* - A_1^* A_5)}{\partial A_1} = -2A_5, \text{ etc.}, \quad (2.22a, b)$$

$$\frac{\partial (A_1 F_x^* + A_1^* F_x)}{\partial A_1} = 2F_x, \text{ etc.} \quad (2.22c)$$

One then finds for the derivatives of Φ

$$\frac{\partial \Phi}{\partial A_1} = \frac{1}{2} \omega^2 \rho h_x h_y A_1 - \frac{1}{2} h_x h_y G (k_z^2 A_1 - i k_z A_5) + \frac{1}{2} F_x, \quad (2.23a)$$

$$\frac{\partial \Phi}{\partial A_2} = \frac{1}{2} \omega^2 \rho h_x h_y A_2 - \frac{1}{2} h_x h_y G (k_z^2 A_2 - i k_z A_6) + \frac{1}{2} F_y, \quad (2.23b)$$

$$\frac{\partial \Phi}{\partial A_3} = \frac{1}{2} \omega^2 \rho h_x h_y A_3 - \frac{1}{2} h_x h_y E k_z^2 A_3 + \frac{1}{2} F_z, \quad (2.23c)$$

$$\frac{\partial \Phi}{\partial A_4} = \frac{1}{2} \omega^2 \rho h_x h_y \left(\frac{h_x^2}{12} + \frac{h_y^2}{12} \right) A_4 - \frac{1}{2} h_x h_y G k_z^2 \left(\frac{h_x^2}{12} + \frac{h_y^2}{12} \right) A_4 + \frac{1}{2} (-F_x y' + F_y x'), \quad (2.23d)$$

$$\frac{\partial \Phi}{\partial A_5} = \frac{1}{2} \omega^2 \rho h_x h_y \frac{h_x^2}{12} A_5 - \frac{1}{2} h_x h_y E k_z^2 \frac{h_x^2}{12} A_5 - \frac{1}{2} h_x h_y G (A_5 + i k_z A_1) + \frac{1}{2} F_z x', \quad (2.23e)$$

$$\frac{\partial \Phi}{\partial A_6} = \frac{1}{2} \omega^2 \rho h_x h_y \frac{h_y^2}{12} A_6 - \frac{1}{2} h_x h_y E k_z^2 \frac{h_y^2}{12} A_6 - \frac{1}{2} h_x h_y G (A_6 + i k_z A_2) + \frac{1}{2} F_z y'. \quad (2.23f)$$

A set of linear equations for the amplitudes, with the external forces forming the right-hand side, is obtained when the derivatives (2.23) are set equal to zero:

$$h_x h_y (\omega^2 \rho - G k_z^2) A_1 + h_x h_y G i k_z A_5 = -F_x, \quad (2.24a)$$

$$h_x h_y (\omega^2 \rho - G k_z^2) A_2 + h_x h_y G i k_z A_6 = -F_y, \quad (2.24b)$$

$$h_x h_y (\omega^2 \rho - E k_z^2) A_3 = -F_z, \quad (2.24c)$$

$$h_x h_y \left(\frac{h_x^2}{12} + \frac{h_y^2}{12} \right) (\omega^2 \rho - G k_z^2) A_4 = F_x y' - F_y x', \quad (2.24d)$$

$$h_x h_y \left(\omega^2 \rho \frac{h_x^2}{12} - E k_z^2 \frac{h_x^2}{12} - G \right) A_5 - h_x h_y G i k_z A_1 = -F_z x', \quad (2.24e)$$

$$h_x h_y \left(\omega^2 \rho \frac{h_y^2}{12} - E k_z^2 \frac{h_y^2}{12} - G \right) A_6 - h_x h_y G i k_z A_2 = -F_z y'. \quad (2.24f)$$

The matrix of this set of equations is relatively sparse, so the solutions can be obtained analytically. The results are

$$A_1 = \frac{-F_x (\omega^2 \rho (h_x^2/12) - G - E k_z^2 (h_x^2/12)) + F_z x' G i k_z}{(E G h_x^3 h_y / 12) (k_z^2 - k_{Bx}^2) (k_z^2 + k_{Nx}^2)}, \quad (2.25a)$$

$$A_2 = \frac{-F_y(\omega^2 \rho (h_y^2/12) - G - Ek_z^2 (h_y^2/12)) + F_z y' G i k_z}{(EGh_y^3 h_x/12)(k_z^2 - k_{By}^2)(k_z^2 + k_{Ny}^2)}, \tag{2.25b}$$

$$A_3 = \frac{F_z}{Eh_x h_y (k_z^2 - k_C^2)}, \tag{2.25c}$$

$$A_4 = \frac{-y' F_x + x' F_y}{Gh_x h_y ((h_x^2/12) + (h_y^2/12))(k_z^2 - k_T^2)}, \tag{2.25d}$$

$$A_5 = \frac{-F_x i k_z + F_z x' (k_z^2 - k_T^2)}{E(h_x^3 h_y/12)(k_z^2 - k_{Bx}^2)(k_z^2 + k_{Nx}^2)}, \tag{2.25e}$$

$$A_6 = \frac{-F_y i k_z + F_z y' (k_z^2 - k_T^2)}{E(h_y^3 h_x/12)(k_z^2 - k_{By}^2)(k_z^2 + k_{Ny}^2)}. \tag{2.25f}$$

As can be seen, the amplitudes are dependent on the wave number k_z of the external force distribution. A number of abbreviations have been used in equations (2.25) to denote the various free wave numbers of a Timoshenko beam. They are

$$k_C = \omega \sqrt{\frac{\rho}{E}} \quad (\text{compressional wave}), \tag{2.26a}$$

$$k_T = \omega \sqrt{\frac{\rho}{G}} \quad (\text{torsional wave, also shear wave}), \tag{2.26b}$$

$$k_{Bx} = \sqrt{\frac{1}{2} \left\{ k_C^2 + k_T^2 + \sqrt{(k_C^2 + k_T^2)^2 - 4k_C^2 \left(k_T^2 - \frac{12}{h_x^2} \right)} \right\}}, \tag{2.26c}$$

$$k_{By} = \sqrt{\frac{1}{2} \left\{ k_C^2 + k_T^2 + \sqrt{(k_C^2 + k_T^2)^2 - 4k_C^2 \left(k_T^2 - \frac{12}{h_y^2} \right)} \right\}} \tag{2.26d}$$

(propagating component of the bending wave with displacement in the x and y direction, respectively),

$$k_{Nx} = \sqrt{\frac{1}{2} \left\{ \sqrt{(k_C^2 + k_T^2)^2 - 4k_C^2 \left(k_T^2 - \frac{12}{h_x^2} \right)} - (k_C^2 + k_T^2) \right\}}, \tag{2.26e}$$

$$k_{Ny} = \sqrt{\frac{1}{2} \left\{ \sqrt{(k_C^2 + k_T^2)^2 - 4k_C^2 \left(k_T^2 - \frac{12}{h_y^2} \right)} - (k_C^2 + k_T^2) \right\}}. \tag{2.26f}$$

k_{Nx} and k_{Ny} are not wave numbers, but the spatial decay rates of the near field of the bending wave with displacement in the x and y direction respectively. They are real for small frequencies, but become imaginary beyond the frequency where the torsional wavelength becomes comparable to the beam thickness [15, p. 290]; this is a feature of a Timoshenko beam that does not occur in an Euler beam.

If equations (2.25a–f) are combined with equation (2.4a–f), the beam’s response to the loading with z -dependence $e^{ik_z(z-z')}$ is fully determined.

The analysis in section 2.2 has been simplified by restricting it to a rectangular beam, which has a doubly symmetric cross-section. As a result, when the beam is unsupported, no

coupling can exist between wave motion in any of the three linear directions and the torsional rotation direction. This leads to the simplicity of equations (2.24). The equations would be much more complicated if the cross-section had no axes of symmetry.

2.3. BEAM RESPONSE TO A POINT FORCE

A point force located at position z' can be written in terms of the δ -function, which in turn can be written in terms of its Fourier integral,

$$\mathbf{F}\delta(z - z') = \frac{\mathbf{F}}{2\pi} \int_{-\infty}^{\infty} e^{ik_z(z-z')} dk_z, \tag{2.27}$$

where \mathbf{F} is the force vector with components F_x, F_y, F_z . The integral in equation (2.27) represents a superposition of forces with distributions that have been considered in the previous section; hence the displacements and angles resulting from the point force can be represented by an equivalent superposition, e.g.,

$$\xi_M = \frac{1}{2\pi} \int_{-\infty}^{\infty} A_1(k_z) e^{ik_z(z-z')} dk_z, \tag{2.28}$$

The amplitudes A_1 - A_6 depend on the wave number k_z and have singularities at the free wave numbers specified in equations (2.26); this leads to singularities in the integrand. Integrals of this type can be calculated with the calculus of residues. Two types of integrals occur. The first is

$$I = \frac{1}{2\pi} \int_{-\infty}^{\infty} \frac{e^{ik_z(z-z')}}{k_z^2 - k_T^2} dk_z, \tag{2.29}$$

and an equivalent integral with k_C in place of k_T . The calculation of this integral is shown in reference [14, pp. 415-416], and the result is

$$I = \frac{i}{2k_T} e^{ik_T|z-z'|}. \tag{2.30}$$

This represents diverging waves, travelling away from the point z' where the excitation is located. The second integral is

$$J = \frac{1}{2\pi} \int_{-\infty}^{\infty} \frac{f(k_z) e^{ik_z(z-z')}}{(k_z^2 - k_{Bx}^2)(k_z^2 + k_{Nx}^2)} dk_z, \tag{2.31}$$

and an equivalent integral with k_{By} and k_{Ny} in place of k_{Bx} and k_{Nx} . $f(k_z)$ stands for a constant, or a linear or quadratic function of k_z . $f(k_z)$ is either even or odd. The calculation of J is shown explicitly in Appendix A. The result is

$$J = \begin{cases} \frac{i}{2(k_{Bx}^2 + k_{Nx}^2)} \left[\frac{f(k_{Bx}) e^{ik_{Bx}|z-z'|}}{k_{Bx}} - \frac{f(ik_{Nx}) e^{-k_{Nx}|z-z'|}}{ik_{Nx}} \right] & \text{for even } f(k_z) \\ \frac{i \operatorname{sgn}(z-z')}{2(k_{Bx}^2 + k_{Nx}^2)} \left[\frac{f(k_{Bx}) e^{ik_{Bx}|z-z'|}}{k_{Bx}} - \frac{f(ik_{Nx}) e^{-k_{Nx}|z-z'|}}{ik_{Nx}} \right] & \text{for odd } f(k_z) \end{cases} \tag{2.32}$$

The expressions in equation (2.32) consist of a propagating wave and a near field. Both diverge from the point z' .

The integrals, such as equation (2.28), of the amplitudes A_1 - A_6 can now be calculated, by using equations (2.30) and (2.32). The results are

$$\begin{aligned} \xi_M = & \frac{F_x}{EGh_x^3 h_y/12} \frac{-i}{2(k_{B_x}^2 + k_{N_x}^2)} \left[\frac{(\omega^2 \rho h_x^2/12 - G - Ek_{B_x}^2 h_x^2/12) e^{ik_{B_x}|z-z'|}}{k_{B_x}} \right. \\ & \left. + \frac{(\omega^2 \rho h_x^2/12 - G + Ek_{N_x}^2 h_x^2/12) e^{-k_{N_x}|z-z'|}}{-ik_{N_x}} \right] \\ & + \frac{F_z x'}{Eh_x^3 h_y/12} \frac{\text{sgn}(z-z')}{2(k_{B_x}^2 + k_{N_x}^2)} \left[-e^{ik_{B_x}|z-z'|} + e^{-k_{N_x}|z-z'|} \right], \end{aligned} \tag{2.33a}$$

$$\begin{aligned} \eta_M = & \frac{F_y}{EGh_y^3 h_x/12} \frac{-i}{2(k_{B_y}^2 + k_{N_y}^2)} \left[\frac{(\omega^2 \rho h_y^2/12 - G - Ek_{B_y}^2 h_y^2/12) e^{ik_{B_y}|z-z'|}}{k_{B_y}} \right. \\ & \left. + \frac{(\omega^2 \rho h_y^2/12 - G + Ek_{N_y}^2 h_y^2/12) e^{-k_{N_y}|z-z'|}}{-ik_{N_y}} \right] \\ & + \frac{F_z y'}{Eh_y^3 h_x/12} \frac{\text{sgn}(z-z')}{2(k_{B_y}^2 + k_{N_y}^2)} \left[-e^{ik_{B_y}|z-z'|} + e^{-k_{N_y}|z-z'|} \right], \end{aligned} \tag{2.33b}$$

$$\zeta_M = \frac{F_z}{Eh_x h_y} \frac{i}{2k_C} e^{ik_C|z-z'|}, \tag{2.33c}$$

$$\varphi_{xy} = \frac{-y' F_x + x' F_y}{Gh_x h_y (h_x^2/12 + h_y^2/12)} \frac{i}{2k_T} e^{ik_T|z-z'|}, \tag{2.33d}$$

$$\begin{aligned} \varphi_{xz} = & \frac{F_x}{Eh_x^3 h_y/12} \frac{\text{sgn}(z-z')}{2(k_{B_x}^2 + k_{N_x}^2)} \left[e^{ik_{B_x}|z-z'|} - e^{-k_{N_x}|z-z'|} \right] \\ & + \frac{F_z x'}{Eh_x^3 h_y/12} \frac{-i}{2(k_{B_x}^2 + k_{N_x}^2)} \left[\frac{(k_T^2 - k_{B_x}^2) e^{ik_{B_x}|z-z'|}}{k_{B_x}} + \frac{(k_T^2 + k_{N_x}^2) e^{-k_{N_x}|z-z'|}}{-ik_{N_x}} \right], \end{aligned} \tag{2.33e}$$

$$\begin{aligned} \varphi_{yz} = & \frac{F_y}{Eh_x^3 h_y/12} \frac{\text{sgn}(z-z')}{2(k_{B_y}^2 + k_{N_y}^2)} \left[e^{ik_{B_y}|z-z'|} - e^{-k_{N_y}|z-z'|} \right] \\ & + \frac{F_z y'}{Eh_y^3 h_x/12} \frac{-i}{2(k_{B_y}^2 + k_{N_y}^2)} \left[\frac{(k_T^2 - k_{B_y}^2) e^{ik_{B_y}|z-z'|}}{k_{B_y}} + \frac{(k_T^2 + k_{N_y}^2) e^{-k_{N_y}|z-z'|}}{-ik_{N_y}} \right]. \end{aligned} \tag{2.33f}$$

The displacements (ξ, η, ζ) can be easily obtained by substituting equations (2.33) into equations (2.1). This gives rise to three lengthy equations which show the dependence of (ξ, η, ζ) on the force vector components (F_x, F_y, F_z). The dependence is of the form (2.2), so the elements of the Green function matrix can be read off directly. The results are summarized in the next section.

2.4. ELEMENTS OF THE GREEN FUNCTION MATRIX

The elements of the Green function matrix are composed of free waves of torsion, compression and bending (propagating and nearfield) in the x and y directions. These free waves propagate along the beam away from the excitation point z' . Their amplitudes are denoted by g with an upper-case subscript, which indicates the wave type, and two lower-case subscripts, which refer to the matrix element; for example, g_{Txx} is the amplitude of the torsional wave occurring in the matrix element G_{xx} . Some of the free-wave amplitudes are co-ordinate dependent; such a dependence is indicated by the relevant arguments.

The elements of the Green function matrix are listed below, together with the amplitudes of the relevant free waves:

$$G_{xx}(\mathbf{r}; \mathbf{r}') = g_{Bxx} e^{ik_{Bx}|z-z'|} + g_{Nxx} e^{-k_{Nx}|z-z'|} + g_{Txx}(y; y') e^{ik_T|z-z'|}, \quad (2.34a)$$

with

$$g_{Bxx} = \frac{12}{EGh_x^3 h_y} \frac{-i}{2(k_{Bx}^2 + k_{Nx}^2)} \frac{\omega^2 \rho h_x^2/12 - G - Ek_{Bx}^2 h_x^2/12}{k_{Bx}}, \quad (2.34b)$$

$$g_{Nxx} = \frac{12}{EGh_x^3 h_y} \frac{-i}{2(k_{Bx}^2 + k_{Nx}^2)} \frac{\omega^2 \rho h_x^2/12 - G + Ek_{Nx}^2 h_x^2/12}{-ik_{Nx}}, \quad (2.34c)$$

$$g_{Txx}(y; y') = \frac{yy'}{Gh_x h_y (h_x^2/12 + h_y^2/12)} \frac{i}{2k_T}. \quad (2.34d)$$

$$G_{xy}(\mathbf{r}; \mathbf{r}') = g_{Txy}(x; y; x', y') e^{ik_T|z-z'|}, \quad (2.35a)$$

with

$$g_{Txy}(x; y; x', y') = \frac{-yx'}{Gh_x h_y (h_x^2/12 + h_y^2/12)} \frac{i}{k_T}. \quad (2.35b)$$

$$G_{xz}(\mathbf{r}; \mathbf{r}') = g_{Bxz}(x; x') \operatorname{sgn}(z-z') e^{ik_{Bx}|z-z'|} + g_{Nxz}(x; x') \operatorname{sgn}(z-z') e^{-k_{Nx}|z-z'|}, \quad (2.36a)$$

with

$$g_{Bxz}(x; x') = \frac{-x'}{Eh_x^3 h_y/12} \frac{1}{2(k_{Bx}^2 + k_{Nx}^2)}, \quad (2.36b)$$

$$g_{Nxz}(x; x') = -g_{Bxz}(x; x'). \quad (2.36c)$$

$$G_{yx}(\mathbf{r}; \mathbf{r}') = g_{Tyx}(x; y; x', y') e^{ik_T|z-z'|}, \quad (2.37a)$$

with

$$g_{Tyx}(x; y; x', y') = \frac{-xy'}{Gh_x h_y (h_x^2/12 + h_y^2/12)} \frac{i}{2k_T}. \quad (2.37b)$$

$$G_{yy}(\mathbf{r}; \mathbf{r}') = g_{Byy} e^{ik_{By}|z-z'|} + g_{Nyy} e^{-k_{Ny}|z-z'|} + g_{Tyy}(x; x') e^{ik_T|z-z'|}, \quad (2.38a)$$

with

$$g_{Byy} = \frac{12}{EGh_y^3 h_x} \frac{-i}{2(k_{By}^2 + k_{Ny}^2)} \frac{\omega^2 \rho h_y^2/12 - G - Ek_{By}^2 h_y^2/12}{k_{By}}, \quad (2.38b)$$

$$g_{Nyy} = \frac{12}{EGh_y^3 h_x} \frac{-i}{2(k_{By}^2 + k_{Ny}^2)} \frac{\omega^2 \rho h_y^2/12 - G + Ek_{Ny}^2 h_y^2/12}{-ik_{Ny}}, \quad (2.38c)$$

$$g_{Tyy}(x; x') = \frac{xx'}{Gh_x h_y (h_x^2/12 + h_y^2/12)} \frac{i}{2k_T}. \quad (2.38d)$$

$$G_{yz}(\mathbf{r}; \mathbf{r}') = g_{Byz}(y; y') \operatorname{sgn}(z - z') e^{ik_{By}|z - z'|} + g_{Nyz}(y; y') \operatorname{sgn}(z - z') e^{-k_{Ny}|z - z'|}, \quad (2.39a)$$

with

$$g_{Byz}(y; y') = \frac{-y'}{Eh_y^3 h_x/12} \frac{1}{2(k_{By}^2 + k_{Ny}^2)}, \quad (2.39b)$$

$$g_{Nyz}(y; y') = -g_{Byz}(y; y'). \quad (2.39c)$$

$$G_{zx}(\mathbf{r}; \mathbf{r}') = g_{Bzx}(x; x') \operatorname{sgn}(z - z') e^{ik_{Bx}|z - z'|} + g_{Nzx}(x; x') \operatorname{sgn}(z - z') e^{-k_{Nx}|z - z'|}, \quad (2.40a)$$

with

$$g_{Bzx}(x; x') = \frac{x}{Eh_x^3 h_y/12} \frac{1}{2(k_{Bx}^2 + k_{Nx}^2)}, \quad (2.40b)$$

$$g_{Nzx}(x; x') = -g_{Bzx}(x; x'). \quad (2.40c)$$

$$G_{zy}(\mathbf{r}; \mathbf{r}') = g_{Bzy}(y; y') \operatorname{sgn}(z - z') e^{ik_{By}|z - z'|} + g_{Nzy}(y; y') \operatorname{sgn}(z - z') e^{-k_{Ny}|z - z'|}, \quad (2.41a)$$

with

$$g_{Bzy}(y; y') = \frac{y}{Eh_y^3 h_x/12} \frac{1}{2(k_{By}^2 + k_{Ny}^2)}, \quad (2.41b)$$

$$g_{Nzy}(y; y') = -g_{Bzy}(y; y'). \quad (2.41c)$$

$$G_{zz}(\mathbf{r}; \mathbf{r}') = g_{Czz} e^{ik_C|z - z'|} + g_{Bzz}^{(x)}(x; x') e^{ik_{Bx}|z - z'|} + g_{Nzz}^{(x)}(x; x') e^{-k_{Nx}|z - z'|} \\ + g_{Bzz}^{(y)}(y; y') e^{ik_{By}|z - z'|} + g_{Nzz}^{(y)}(y; y') e^{-k_{Ny}|z - z'|}, \quad (2.42a)$$

with

$$g_{Czz} = \frac{1}{Eh_x h_y} \frac{i}{2k_C}, \quad (2.42b)$$

$$g_{Bzz}^{(x)}(x; x') = \frac{-xx'}{Eh_x^3 h_y/12} \frac{i}{2(k_{Bx}^2 + k_{Nx}^2)} \frac{k_T^2 - k_{Bx}^2}{k_{Bx}}, \quad (2.42c)$$

$$g_{Nzz}^{(x)}(x; x') = \frac{-xx'}{Eh_x^3 h_y/12} \frac{i}{2(k_{Bx}^2 + k_{Nx}^2)} \frac{k_T^2 + k_{Nx}^2}{-ik_{Nx}}, \quad (2.42d)$$

$$g_{Bzz}^{(y)}(y; y') = \frac{-yy'}{Eh_y^3 h_x/12} \frac{i}{2(k_{By}^2 + k_{Ny}^2)} \frac{k_T^2 - k_{By}^2}{k_{By}}, \quad (2.42e)$$

$$g_{Nzz}^{(y)}(y; y') = \frac{-yy'}{Eh_y^3 h_x/12} \frac{i}{2(k_{By}^2 + k_{Ny}^2)} \frac{k_T^2 + k_{Ny}^2}{-ik_{Ny}}. \quad (2.42f)$$

The free wave amplitudes satisfy the following relationships:

$$g_{Txx}g_{Tyy} - g_{Tyx}g_{Txy} = 0, \quad g_{Bxx}g_{Bzz}^{(x)} - g_{Bxz}g_{Bzx} = 0, \quad (2.43a, b)$$

$$g_{Nxx}g_{Nzz}^{(x)} - g_{Nxz}g_{Nzx} = 0, \quad g_{Byy}g_{Bzz}^{(y)} - g_{Byz}g_{Bzy} = 0, \quad (2.43c, d)$$

$$g_{Nyy}g_{Nzz}^{(y)} - g_{Nzy}g_{Nyz} = 0. \quad (2.43e)$$

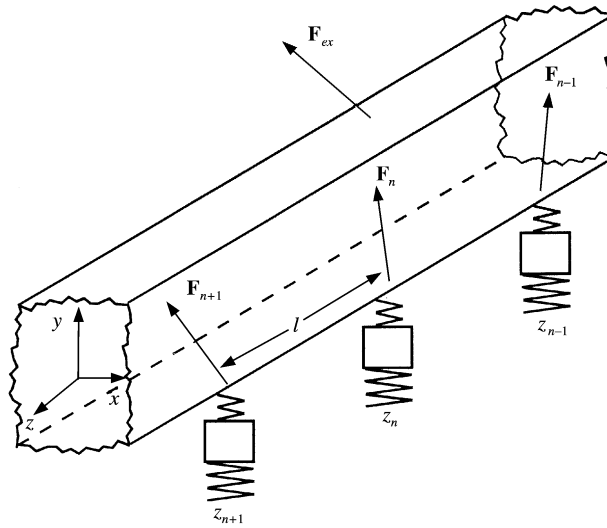


Figure 3. Periodically supported Timoshenko beam.

3. PERIODICALLY SUPPORTED TIMOSHENKO BEAM

3.1. SUPERPOSITION PRINCIPLE

Now a Timoshenko beam is considered, which has infinitely many support points, spaced regularly at positions x_s, y_s, z_n ($n = -\infty, \dots, \infty$) along the beam axis (see Figure 3). The integer n numbers the support points, and $z_n = n\ell$, where ℓ is the distance between adjacent support points. These supports exert forces \mathbf{F}_n with components F_{nx}, F_{ny}, F_{nz} of the beam. Apart from these forces, there is also an external force, \mathbf{F}_{ex} at point (x_{ex}, y_{ex}, z_{ex}) .

The beam motion can be described by applying the superposition principle (see also reference [16]) which states that the response from all sleeper points and from the external point force add up linearly to give the total response. The individual responses can be expressed in terms of Green functions (see equation (2.2)), and one obtains for the lateral, vertical and axial motion

$$\begin{aligned}
 \begin{bmatrix} \xi(z) \\ \eta(z) \\ \zeta(z) \end{bmatrix} &= \sum_{n=-\infty}^{\infty} \begin{bmatrix} G_{xx}(z; z_n) & G_{xy}(z; z_n) & G_{xz}(z; z_n) \\ G_{yx}(z; z_n) & G_{yy}(z; z_n) & G_{yz}(z; z_n) \\ G_{zx}(z; z_n) & G_{zy}(z; z_n) & G_{zz}(z; z_n) \end{bmatrix} \begin{bmatrix} F_{nx} \\ F_{ny} \\ F_{nz} \end{bmatrix} \\
 &+ \begin{bmatrix} G_{xx}(z; z_{ex}) & G_{xy}(z; z_{ex}) & G_{xz}(z; z_{ex}) \\ G_{yx}(z; z_{ex}) & G_{yy}(z; z_{ex}) & G_{yz}(z; z_{ex}) \\ G_{zx}(z; z_{ex}) & G_{zy}(z; z_{ex}) & G_{zz}(z; z_{ex}) \end{bmatrix} \begin{bmatrix} F_x^{ex} \\ F_y^{ex} \\ F_z^{ex} \end{bmatrix}. \tag{3.1}
 \end{aligned}$$

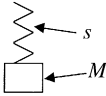
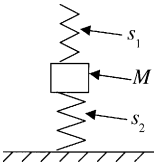
For ease of notation, x and y have been dropped from the arguments and only the z -dependence is explicitly stated.

The forces at the support points are reactive forces and can be related by an impedance to the corresponding displacement,

$$F_{nx} = -Z_x \xi(z_n), \quad F_{ny} = -Z_y \eta(z_n), \quad F_{nz} = -Z_z \zeta(z_n). \tag{3.2a-c}$$

TABLE 1

Impedances for some support types; Z = force/displacement

Support type	Impedance	
Mass M	$Z = -M\omega^2$	
Spring with stiffness s	$Z = s$	
Mass/spring system	$Z = \frac{M\omega^2 s}{M\omega^2 - s}$	
Spring/mass/spring system	$Z = \frac{M\omega^2 s_1 - s_1 s_2}{M\omega^2 - (s_1 + s_2)}$	

The impedances can represent any type of support, such as masses, springs or combinations of masses and springs. Examples are given in Table 1. Damping caused by the loss factor of a spring can be introduced using a complex stiffness.

Equations (3.1) and (3.2) can be combined. If the resulting equation is evaluated at all support points z_m , it represents a linear set of equations for the displacements $\xi(z_m), \eta(z_m), \zeta(z_m)$. These equations will be analyzed for the homogeneous case, where external forces are absent. This gives the free waves on a periodically supported Timoshenko beam. They are called Bloch waves here, to avoid confusion with the free waves on a beam without supports. The non-homogeneous case, which is not considered further in this paper, leads to results for the receptances.

3.2. BLOCH WAVES ON A PERIODICALLY SUPPORTED BEAM

The Bloch waves considered here are governed by the homogeneous version of equation (3.1),

$$\xi(z_m) + \sum_{n=-\infty}^{\infty} [Z_x G_{xx}(z_m; z_n)\xi(z_n) + Z_y G_{xy}(z_m; z_n)\eta(z_n) + Z_z G_{xz}(z_m; z_n)\zeta(z_n)] = 0, \quad (3.3a)$$

$$\eta(z_m) + \sum_{n=-\infty}^{\infty} [Z_x G_{yx}(z_m; z_n)\xi(z_n) + Z_y G_{yy}(z_m; z_n)\eta(z_n) + Z_z G_{yz}(z_m; z_n)\zeta(z_n)] = 0, \quad (3.3b)$$

$$\zeta(z_m) + \sum_{n=-\infty}^{\infty} [Z_x G_{zx}(z_m; z_n)\xi(z_n) + Z_y G_{zy}(z_m; z_n)\eta(z_n) + Z_z G_{zz}(z_m; z_n)\zeta(z_n)] = 0. \quad (3.3c)$$

Bloch's theorem [17] states that the free waves in a 1-D periodic system with repeat length ℓ propagate in such a way that the associated field quantities have a spatial dependence $e^{-\gamma m \ell}$ (m is an integer). γ is the Bloch propagation constant; it is generally complex,

$$\gamma = \alpha - ik, \quad (3.4)$$

where α is the attenuation of waves in the periodic system, and k is the Bloch wave number. This implies for the three displacements considered here

$$\xi(z_m) = \xi_0 e^{-\gamma z_m}, \quad \eta(z_m) = \eta_0 e^{-\gamma z_m}, \quad \zeta(z_m) = \zeta_0 e^{-\gamma z_m} \quad (3.5a-c)$$

and equivalent expressions for the displacements at z_n . ξ_0, η_0 and ζ_0 are amplitudes.

Substitution of equation (3.5) and the Green functions of equations (2.34a), (2.35a), ..., (2.42a) into equations (3.3) leads to

$$\begin{aligned} & \xi_0 e^{-\gamma m \ell} + Z_x \sum_{n=-\infty}^{\infty} [g_{Bxx} e^{ik_{Bx}|m-n|\ell} + g_{Nxx} e^{-k_{Nx}|m-n|\ell} + g_{Txx} e^{ik_T|m-n|\ell}] \xi_0 e^{-\gamma n \ell} \\ & + Z_y \sum_{n=-\infty}^{\infty} g_{Txy} e^{ik_T|m-n|\ell} \eta_0 e^{-\gamma n \ell} \\ & + Z_z \sum_{n=-\infty}^{\infty} [g_{Bxz} e^{ik_{Bx}|m-n|\ell} + g_{Nxz} e^{-k_{Nx}|m-n|\ell}] \operatorname{sgn}(m-n) \zeta_0 e^{-\gamma n \ell} = 0, \end{aligned} \quad (3.6a)$$

$$\begin{aligned} & Z_x \sum_{n=-\infty}^{\infty} g_{Tyx} e^{ik_T|m-n|\ell} \xi_0 e^{-\gamma n \ell} \\ & + \eta_0 e^{-\gamma m \ell} + Z_y \sum_{n=-\infty}^{\infty} [g_{Byy} e^{ik_{By}|m-n|\ell} + g_{Nyy} e^{-k_{Ny}|m-n|\ell} + g_{Tyy} e^{ik_T|m-n|\ell}] \eta_0 e^{-\gamma n \ell} \\ & + Z_z \sum_{n=-\infty}^{\infty} [g_{Byz} e^{ik_{By}|m-n|\ell} + g_{Nyz} e^{-k_{Ny}|m-n|\ell}] \operatorname{sgn}(m-n) \zeta_0 e^{-\gamma n \ell} = 0, \end{aligned} \quad (3.6b)$$

$$\begin{aligned} & Z_x \sum_{n=-\infty}^{\infty} [g_{Bzx} e^{ik_{Bx}|m-n|\ell} + g_{Nzx} e^{-k_{Nx}|m-n|\ell}] \operatorname{sgn}(m-n) \xi_0 e^{-\gamma n \ell} \\ & + Z_y \sum_{n=-\infty}^{\infty} [g_{Bzy} e^{ik_{By}|m-n|\ell} + g_{Nzy} e^{-k_{Ny}|m-n|\ell}] \operatorname{sgn}(m-n) \eta_0 e^{-\gamma n \ell} \\ & + \zeta_0 e^{-\gamma m \ell} + Z_z \sum_{n=-\infty}^{\infty} [g_{Czz} e^{ik_C|m-n|\ell} + g_{Bzz}^{(x)} e^{ik_{Bx}|m-n|\ell} + g_{Nzz}^{(x)} e^{-k_{Nx}|m-n|\ell} \\ & + g_{Bzz}^{(y)} e^{ik_{By}|m-n|\ell} + g_{Nzz}^{(y)} e^{-k_{Ny}|m-n|\ell}] \zeta_0 e^{-\gamma n \ell} = 0. \end{aligned} \quad (3.6c)$$

Multiplication of all three equations by $e^{\gamma m \ell}$ and change of the summation index from $m-n$ to n , gives equations with sums that are combinations of geometric series. These sums can hence be evaluated:

$$\sum_{n=-\infty}^{\infty} e^{\gamma n \ell} e^{ik|n|\ell} = \frac{-i \sin k \ell}{\cos k \ell - \cosh \gamma \ell}, \quad (3.7a)$$

$$\sum_{n=-\infty}^{\infty} \operatorname{sgn}(n) e^{\gamma n \ell} e^{ik|n|\ell} = \frac{\sinh k \ell}{\cos k \ell - \cosh \gamma \ell}, \quad (3.7b)$$

$$\sum_{n=-\infty}^{\infty} e^{\gamma n \ell} e^{-k|n|\ell} = \frac{\sinh k \ell}{\cosh k \ell - \cosh \gamma \ell}, \quad (3.7c)$$

$$\sum_{n=-\infty}^{\infty} \operatorname{sgn}(n) e^{\gamma n \ell} e^{-k|n|\ell} = \frac{\sinh \gamma \ell}{\cosh k \ell - \cosh \gamma \ell}. \quad (3.7d)$$

In equations (3.7a) and (3.7b), k stands for any of the wave numbers k_{Bx}, k_{By}, k_T, k_C ; in equations (3.7c) and (3.7d), k stands for k_{Nx} or k_{Ny} .

Equations (3.6) become, after use of equations (3.7),

$$\begin{bmatrix} a_{11} & a_{12} & a_{13} \\ a_{21} & a_{22} & a_{23} \\ a_{31} & a_{32} & a_{33} \end{bmatrix} \begin{bmatrix} \zeta_0 \\ \eta_0 \\ \zeta_0 \end{bmatrix} = 0, \tag{3.8}$$

with

$$a_{11} = 1 + Z_x \left[g_{Bxx} \frac{-i \sin k_{Bx}\ell}{\cos k_{Bx}\ell - \cosh \gamma\ell} + g_{Nxx} \frac{\sinh k_{Nx}\ell}{\cosh k_{Nx}\ell - \cosh \gamma\ell} + g_{Txx} \frac{-i \sin k_T\ell}{\cos k_T\ell - \cosh \gamma\ell} \right], \tag{3.9a}$$

$$a_{12} = Z_y g_{Txy} \frac{-i \sin k_T\ell}{\cos k_T\ell - \cosh \gamma\ell}, \tag{3.9b}$$

$$a_{13} = Z_z \left[g_{Bxz} \frac{\sinh \gamma\ell}{\cos k_{Bx}\ell - \cosh \gamma\ell} + g_{Nxz} \frac{\sinh \gamma\ell}{\cosh k_{Nx}\ell - \cosh \gamma\ell} \right], \tag{3.9c}$$

$$a_{21} = Z_x g_{Tyx} \frac{-i \sin k_T\ell}{\cos k_T\ell - \cosh \gamma\ell}, \tag{3.9d}$$

$$a_{22} = 1 + Z_y \left[g_{Byy} \frac{-i \sin k_{By}\ell}{\cos k_{By}\ell - \cosh \gamma\ell} + g_{Nyy} \frac{\sinh k_{Ny}\ell}{\cosh k_{Ny}\ell - \cosh \gamma\ell} + g_{Ty y} \frac{-i \sin k_T\ell}{\cos k_T\ell - \cosh \gamma\ell} \right], \tag{3.9e}$$

$$a_{23} = Z_z \left[g_{Byz} \frac{\sinh \gamma\ell}{\cos k_{By}\ell - \cosh \gamma\ell} + g_{Nyz} \frac{\sinh \gamma\ell}{\cosh k_{Ny}\ell - \cosh \gamma\ell} \right], \tag{3.9f}$$

$$a_{31} = Z_x \left[g_{Bzx} \frac{\sinh \gamma\ell}{\cos k_{Bx}\ell - \cosh \gamma\ell} + g_{Nzx} \frac{\sinh \gamma\ell}{\cosh k_{Nx}\ell - \cosh \gamma\ell} \right], \tag{3.9g}$$

$$a_{32} = Z_y \left[g_{Bzy} \frac{\sinh \gamma\ell}{\cos k_{By}\ell - \cosh \gamma\ell} + g_{Nzy} \frac{\sinh \gamma\ell}{\cosh k_{Ny}\ell - \cosh \gamma\ell} \right], \tag{3.9h}$$

$$a_{33} = 1 + Z_z \left[g_{Czz} \frac{-i \sin k_C\ell}{\cos k_C\ell - \cosh \gamma\ell} + g_{Bzz}^{(x)} \frac{-i \sin k_{Bx}\ell}{\cos k_{Bx}\ell - \cosh \gamma\ell} + g_{Nzz}^{(x)} \frac{\sinh k_{Nx}\ell}{\cosh k_{Nx}\ell - \cosh \gamma\ell} \right. \\ \left. + g_{Bzz}^{(y)} \frac{-i \sin k_{By}\ell}{\cos k_{By}\ell - \cosh \gamma\ell} + g_{Nzz}^{(y)} \frac{\sinh k_{Ny}\ell}{\cosh k_{Ny}\ell - \cosh \gamma\ell} \right]. \tag{3.9i}$$

Equation (3.8) is a homogeneous linear set of equations and has non-trivial solutions only if its determinant vanishes,

$$\det \mathbf{A} = 0, \tag{3.10}$$

where \mathbf{A} stands for the 3×3 matrix in equation (3.8). When expanded, using expressions (3.9a-i) for the matrix elements, this determinant condition contains terms $\cosh \gamma\ell$ and $\sinh \gamma\ell$, and is thus an implicit equation for the unknown Bloch wave number γ . This equation contains several denominators originating from the use of equations (3.7). This

indicates that γ cannot take values such that $\cosh \gamma\ell = \cos k\ell$ (k stands for k_{Bx}, k_{By}, k_T, k_C) or $\cosh \gamma\ell = \cosh k\ell$ (k stands for k_{Nx} or k_{Ny}).

In order to solve for $\cosh \gamma\ell$ numerically, the expanded version of equation (3.10) is multiplied by all denominators occurring in it. Further, $\sinh^2 \gamma\ell = \cosh^2 \gamma\ell - 1$ is used to substitute for $\sinh \gamma\ell$, and one then obtains a polynomial equation of 11th degree in $\cosh \gamma\ell$. The degree 11 of the polynomial suggests that there are 11 roots for $\cosh \gamma\ell$. This seems to contradict the result of Mead [8], who found that the number of roots is equal to the number of coupling co-ordinates. Here there are six coupling co-ordinates (the three centreline displacements and three angles appearing in equation (2.1)), so the extra five roots must be spurious. It can be shown that the extra five solutions are $\cos k_T\ell, \cos k_{Bx}\ell, \cosh k_{Nx}\ell, \cos k_{By}\ell, \cosh k_{Ny}\ell$, which have been excluded by the argument in the previous paragraph. They are merely an artefact of multiplying equation (3.10) by the denominators in equations (3.9a-i). Thus, the number of solutions is reconciled with Mead's findings.

Once all six solutions for $\cosh \gamma\ell$ have been found, the Bloch wave number γ can be determined from the inverse of the hyperbolic cosine,

$$\gamma\ell = \ln(\cosh \gamma\ell + \sqrt{\cosh^2 \gamma\ell - 1}) = \ln|\Gamma| + i \arctan \left(\frac{\text{Im}(\Gamma)}{\text{Re}(\Gamma)} + 2\pi v \right), \quad (3.11a)$$

where

$$\Gamma = \cosh \gamma\ell + \sqrt{\cosh^2 \gamma\ell - 1}. \quad (3.11b)$$

The first part of equation (3.11a) is based on equation (4.6.21), and the second part of equation (3.11a) on equation (4.1.5) in reference [18].

There are infinitely many solutions ($v = 0, \pm 1, \pm 2, \dots$) differing by integer multiples of 2π . Only the case $v = 0$ will be considered.

Equation (3.8) includes all six wave types that can occur on the beam. There may be cases where fewer than six wave types are present, and such cases are described by reduced versions of equation (3.8). Some such cases are considered below.

3.2.1. Compressional waves

This section considers the case where only compressional waves are present on the beam. The absence of all other waves can be simulated by setting to zero all Green function components, except for g_{Czz} . The matrix in equation (3.8) then reduces to

$$\mathbf{A} = \begin{bmatrix} 1 & 0 & 0 \\ 0 & 1 & 0 \\ 0 & 0 & a_{33} \end{bmatrix}, \quad (3.12)$$

with

$$a_{33} = 1 + Z_z g_{Czz} \frac{-i \sin k_C \ell}{\cos k_C \ell - \cosh \gamma\ell}. \quad (3.13)$$

The determinant condition (3.10) gives

$$a_{33} = 0, \quad (3.14)$$

from which

$$\cosh \gamma\ell = \cos k_C \ell - Z_z g_{Czz} i \sin k_C \ell \quad (3.15)$$

can be derived easily. This is a polynomial of first degree, and there is one root for $\cosh \gamma\ell$. An equation equivalent to equation (3.15) with a mass impedance has been found by earlier authors; see, e.g., reference [15, section 5.5.2].

3.2.2. *Torsional waves*

This section considers the case where only torsional waves with a displacement in the xy -plane are present on the beam. All Green function components, except for g_{Txx} , g_{Txy} , g_{Tyx} and g_{Tyy} are set to zero in order to simulate the absence of all but the torsional waves. In addition, it is assumed that $(x', y') \neq (0, 0)$, i.e., the support points are offset from the centreline, otherwise the torsional waves would not be affected by the periodic supports. This scenario represents a mathematical idealization, in that it is practically impossible to excite torsional waves while suppressing the coupling of torsional and bending waves on the considered beam/support configuration. The matrix in equation (3.8) then reduces to

$$\mathbf{A} = \begin{bmatrix} a_{11} & a_{12} & 0 \\ a_{21} & a_{22} & 0 \\ 0 & 0 & 1 \end{bmatrix}, \tag{3.16}$$

with

$$a_{11} = 1 + Z_x g_{Txx} \frac{-i \sin k_T \ell}{\cos k_T \ell - \cosh \gamma \ell}, \tag{3.17a}$$

$$a_{12} = Z_x g_{Txy} \frac{-i \sin k_T \ell}{\cos k_T \ell - \cosh \gamma \ell}, \tag{3.17b}$$

$$a_{21} = Z_y g_{Tyx} \frac{-i \sin k_T \ell}{\cos k_T \ell - \cosh \gamma \ell}, \tag{3.17c}$$

$$a_{22} = 1 + Z_y g_{Tyy} \frac{-i \sin k_T \ell}{\cos k_T \ell - \cosh \gamma \ell}. \tag{3.17d}$$

The determinant condition (3.10) gives

$$a_{11} a_{22} - a_{12} a_{21} = 0. \tag{3.18}$$

After a few straightforward manipulations and use of equation (2.43a), a polynomial of second degree for $\cosh \gamma\ell$ is obtained. One root is $\cosh \gamma\ell = \cos k_T \ell$. This solution is not allowed and is excluded by dividing the polynomial by $(\cos k_T \ell - \cosh \gamma\ell)$. The result is

$$\cosh \gamma\ell = \cos k_T \ell - (Z_x g_{Txx} + Z_y g_{Tyy}) i \sin k_T \ell. \tag{3.19}$$

which is of the same structure as the result (3.15) found for purely compressional waves.

3.2.3. *Vertical bending waves*

This section considers the case where only bending waves in the y direction are present on the beam. The absence of all other waves is simulated by setting to zero all Green function components corresponding to these wave types. This leaves g_{Byy} , $g_{Ny y}$, g_{Byz} , $g_{Ny z}$, g_{Bzy} , g_{Nzy} . In order to keep the calculations as simple as possible, it is also assumed that the support points and observer points are at the centreline of the beam ($y' = 0$ and $y = 0$). Then the

only non-zero Green function components are g_{Byy} and g_{Nyy} , and the matrix in equation (3.8) reduces to

$$\mathbf{A} = \begin{bmatrix} 1 & 0 & 0 \\ 0 & a_{22} & 0 \\ 0 & 0 & 1 \end{bmatrix}, \quad (3.20)$$

with

$$a_{22} = 1 + Z_y \left[g_{Byy} \frac{-i \sin k_{By} \ell}{\cos k_{By} \ell - \cosh \gamma \ell} + g_{Nyy} \frac{\sinh k_{Ny} \ell}{\cosh k_{Ny} \ell - \cosh \gamma \ell} \right]. \quad (3.21)$$

The determinant condition (3.10) gives

$$a_{22} = 0, \quad (3.22)$$

from which

$$\begin{aligned} & \cosh^2 \gamma \ell \\ & + \cosh \gamma \ell [-\cosh k_{Ny} \ell - \cos k_{By} \ell + Z_y (g_{Byy} i \sin k_{By} \ell - g_{Nyy} \sinh k_{Ny} \ell)] \\ & + \cos k_{By} \ell \cosh k_{Ny} \ell + Z_y (-i g_{Byy} \sin k_{By} \ell \cosh k_{Ny} \ell + g_{Nyy} \sinh k_{Ny} \ell \cos k_{By} \ell) = 0 \end{aligned} \quad (3.23)$$

can be derived in a straightforward way. This is a polynomial of second degree, and there are two roots for $\cosh \gamma \ell$.

This case, too, has been considered by earlier authors, see, e.g., reference [15, section 5.5.3], where an alternative approach is used.

3.2.4. Horizontal and vertical bending waves

This section considers the case where bending waves with displacements in the x and y direction, but no other wave types, are present on the beam. As in section 3.2.3, it is assumed that the support points are at the centreline of the beam ($x' = 0, y' = 0, x = 0, y = 0$). Then only the Green function components $g_{Bxx}, g_{Nxx}, g_{Byy}, g_{Nyy}$ need to be taken into account. The matrix in equation (3.8) reduces to

$$\mathbf{A} = \begin{bmatrix} a_{11} & 0 & 0 \\ 0 & a_{22} & 0 \\ 0 & 0 & 1 \end{bmatrix}, \quad (3.24)$$

with

$$a_{11} = 1 + Z_x \left[g_{Bxx} \frac{-i \sin k_{Bx} \ell}{\cos k_{Bx} \ell - \cosh \gamma \ell} + g_{Nxx} \frac{\sinh k_{Nx} \ell}{\cosh k_{Nx} \ell - \cosh \gamma \ell} \right], \quad (3.25a)$$

$$a_{22} = 1 + Z_y \left[g_{Byy} \frac{-i \sin k_{By} \ell}{\cos k_{By} \ell - \cosh \gamma \ell} + g_{Nyy} \frac{\sinh k_{Ny} \ell}{\cosh k_{Ny} \ell - \cosh \gamma \ell} \right]. \quad (3.25b)$$

The determinant condition (3.10) gives

$$a_{11} a_{22} = 0, \quad (3.26)$$

from which

$$\begin{aligned} & \{ \cosh^2 \gamma \ell + \cosh \gamma \ell [- \cosh k_{N_x} \ell - \cos k_{B_x} \ell + Z_x (g_{B_{xx}} i \sin k_{B_x} \ell - g_{N_{xx}} \sinh k_{N_x} \ell)] \\ & \quad + \cos k_{B_x} \ell \cosh k_{N_x} \ell + Z_x (- i g_{B_{xx}} \sin k_{B_x} \ell \cosh k_{N_x} \ell + g_{N_{xx}} \sinh k_{N_x} \ell \cos k_{B_x} \ell) \} \\ & \times \{ \cosh^2 \gamma \ell + \cosh \gamma \ell [- \cosh k_{N_y} \ell - \cos k_{B_y} \ell + Z_y (g_{B_{yy}} i \sin k_{B_y} \ell - g_{N_{yy}} \sinh k_{N_y} \ell)] \\ & \quad + \cos k_{B_y} \ell \cosh k_{N_y} \ell + Z_y (- i g_{B_{yy}} \sin k_{B_y} \ell \cosh k_{N_y} \ell + g_{N_{yy}} \sinh k_{N_y} \ell \cos k_{B_y} \ell) \} = 0 \end{aligned} \tag{3.27}$$

can be derived. This represents a product of two second degree polynomials, both of the same form as equation (3.23); equation (3.27) has four roots for $\cosh \gamma \ell$, and as the factorized form of this equation shows, the horizontal and vertical bending waves are uncoupled.

3.2.5. Horizontal/vertical bending and torsional waves

This section considers the case where horizontal bending waves, vertical bending waves and torsional waves propagate along the periodically supported beam. Compressional waves are absent, and this is modelled by setting $g_{Czz} = 0$. All other Green function components are non-zero. In order to keep the calculations as simple as possible, it is also assumed that $Z_z = 0$. In section 3.2.4, the support points were on the centreline of the beam; however, torsional waves would not be affected by such supports, so here the supports are assumed to be off-centre. The matrix \mathbf{A} in the determinant condition (3.10) then reduces to

$$\mathbf{A} = \begin{bmatrix} a_{11} & a_{12} & 0 \\ a_{21} & a_{22} & 0 \\ a_{31} & a_{32} & 1 \end{bmatrix}, \tag{3.28}$$

and this leads to

$$a_{11} a_{22} - a_{12} a_{21} = 0. \tag{3.29}$$

The matrix elements a_{11} , a_{12} , a_{21} and a_{22} are given by the full expressions (3.9a), (3.9b), (3.9d) and (3.9e) respectively. A polynomial of sixth degree for $\cosh \gamma \ell$ can be derived from equation (3.29). The manipulations are best done with an algebraic manipulation package. The degree of the polynomial is 6, but the number of coupling co-ordinates is only 5 (displacements ξ_M and η_M , angles φ_{xy} , φ_{xz} , φ_{yz}). This indicates the presence of a spurious root for $\cosh \gamma \ell$, which has to be excluded. It can be shown that this root is $\cosh \gamma \ell = \cos k_T \ell$, and this root is excluded by an appropriate polynomial division. The result is

$$\cosh^5 \gamma \ell + a_5 \cosh^4 \gamma \ell + b_5 \cosh^3 \gamma \ell + c_5 \cosh^2 \gamma \ell + d_5 \cosh \gamma \ell + e_5 = 0, \tag{3.30}$$

which has five roots, as required. The coefficients a_5 , b_5 , c_5 , d_5 , e_5 are listed in Appendix B.

4. NUMERICAL RESULTS AND DISCUSSION

4.1. PROPERTIES OF THE PERIODICALLY SUPPORTED BEAM

For the numerical calculations, a steel beam is considered with the following material properties: $\rho = 8000 \text{ kg/m}^3$ (mass density), $E = 2 \times 10^{11} \text{ N/m}^2$ (Young's modulus), $\nu = 0.3$

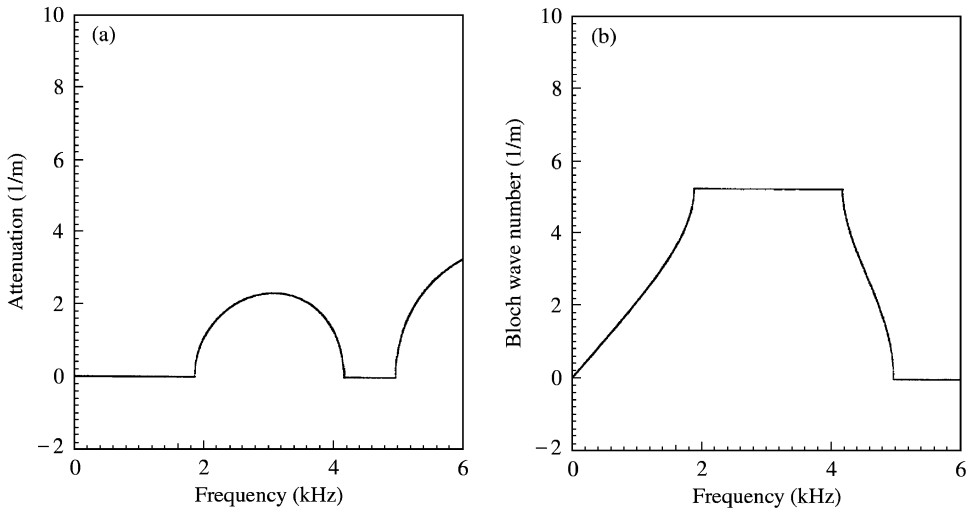


Figure 4. Compressional wave on a beam with mass supports: (a) attenuation spectrum; (b) Bloch wave number spectrum.

(Poisson ratio), and the following geometry: $h_x = 0.09$ m (beam width), $h_y = 0.22$ m (beam height). A beam of this geometry has a lateral and vertical bending stiffness which is similar to that of a typical rail of European railway track.

The supports were spaced a distance $\ell = 0.6$ m apart. Two support types were considered: mass supports with a mass of 162 kg (sleeper mass) and spring supports with stiffnesses $s_x = 10^{10}$ N/m, $s_y = 3 \times 10^{10}$ N/m, $s_z = 10^{10}$ N/m, in the lateral, vertical and axial directions. These support properties, too, are typical of European railway track.

4.2. NUMERICAL RESULTS FOR MASS SUPPORTS

The different combinations of wave types that were the subject of sections 3.2.1–3.2.5, are considered again here.

4.2.1. Compressional waves

The Bloch propagation constant γ was calculated from equation (3.15) and is shown as a function of frequency in Figure 4. Figure 4(a) gives the real part of γ , i.e., the attenuation of the compressional wave; Figure 4(b) gives the imaginary part of γ , i.e., the Bloch wave number. The attenuation spectrum shows bands of zero attenuation (passing bands) alternating with bands of positive attenuation (stopping bands). The width of the bands is related to the ‘‘pinned–pinned frequency’’; this is the frequency where half a wavelength (or an integer multiple of half a wavelength) is equal to the repeat length ℓ . For the compressional wave considered here, the relevant wavelength is $\lambda_c = (2\pi/\omega)\sqrt{E/\rho}$ (from $\lambda_c = 2\pi/k_c$ and equation (2.26a)), yielding a pinned–pinned frequency of 4166 Hz. This is also the upper bound of the first stopping band.

The features in the Bloch wave number spectrum corresponding to passing bands and stopping bands are bands of varying and bands of constant Bloch wave number. The constant values are at $k = 0$ and π/ℓ .

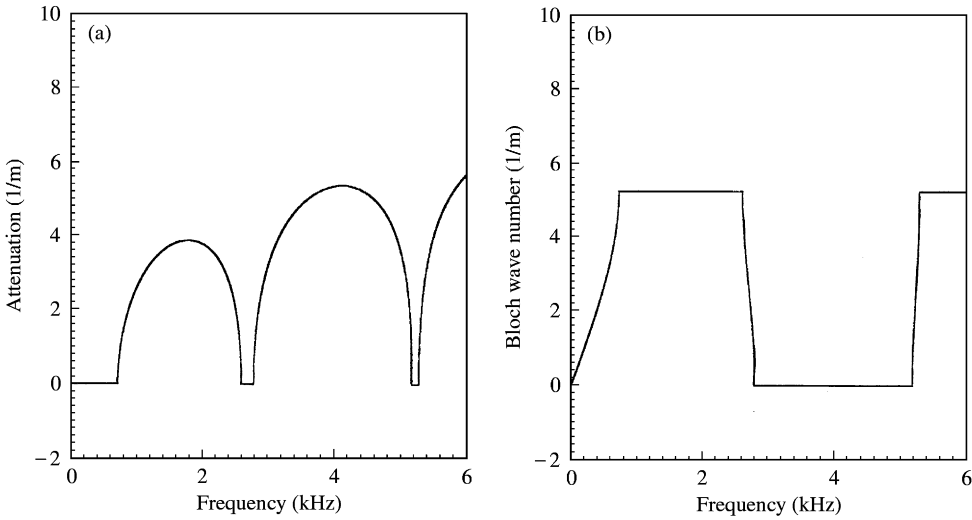


Figure 5. Torsional wave on a beam with mass supports: (a) attenuation spectrum; (b) Bloch wave number spectrum.

4.2.2. Torsional waves

The Bloch propagation constant γ was calculated from equation (3.19) and is shown as a function of frequency in Figure 5. The support points were off the centreline of the beam at $x' = h_x/2$ and $y' = -h_y/2$. The attenuation spectrum (Figure 5(a)) shows alternating passing and stopping bands, where the width of the passing bands decreases with increasing frequency, and the width of the stopping bands increases. The combined width of a passing/stopping band pair, however, is constant and equal to the pinned–pinned frequency, which is 2584 Hz. This value has been calculated by equating half the torsional wavelength, which is $\lambda_T = (2\pi/\omega)\sqrt{G/\rho}$ (from $\lambda_T = 2\pi/k_T$ and equation (2.26b)), to the repeat length ℓ . The spectrum of the Bloch wave number (Figure 5(b)) shows bands of constant values, which are at $k = 0$ and π/ℓ , and bands of varying k , where k varies between the two constant values.

The case of torsional waves is directly analogous to that of the compressional waves and differs only by the scale along the frequency axis. The bands of torsional waves are narrower than those of compressional waves because, at a given frequency, the torsional wavelength is smaller than the compressional wavelength.

4.2.3. Vertical bending waves

The Bloch propagation constant γ was calculated from equation (3.23), and the two solutions are plotted as a function of frequency in Figure 6. The attenuation spectrum (Figure 6(a)) shows that one of the two solutions is always attenuated (reminiscent of the nearfield solution of a free beam without supports), and the other solution shows a passing/stopping band behaviour. The nearfield solution has a Bloch wave number which is zero throughout (see Figure 6(b)), the other solution shows the alternation of varying and constant bands that were observed for compressional and torsional waves. In contrast to compressional and torsional waves, the pinned–pinned frequencies and upper bounds of the stopping bands are not equally spaced, but increase with increasing frequency. Pinned–pinned frequencies are the frequencies where an integer multiple of half a bending

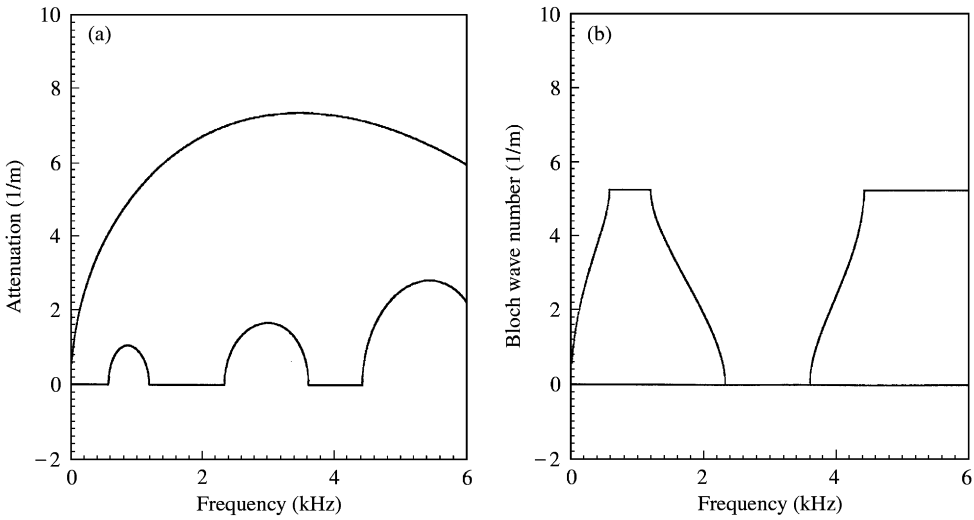


Figure 6. Vertical bending wave on a beam with mass supports: (a) attenuation spectrum; (b) Bloch wave number spectrum.

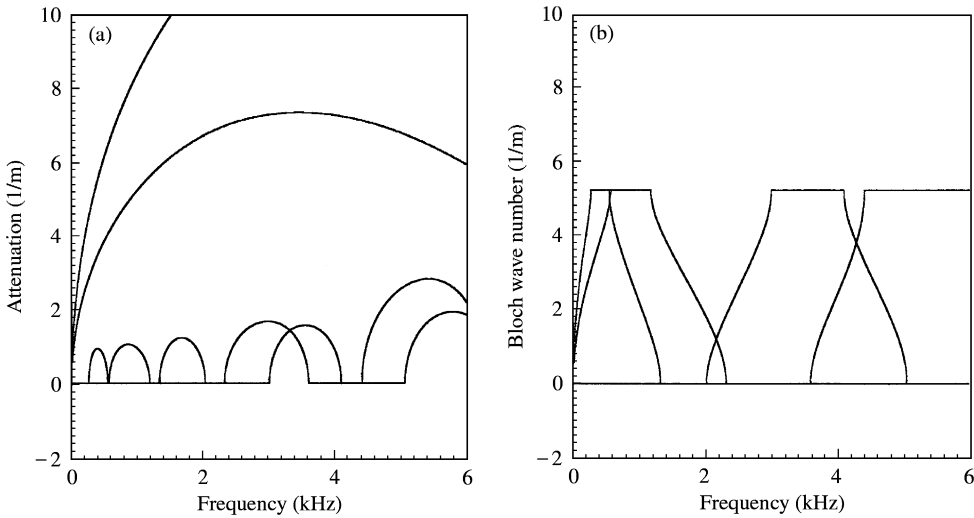


Figure 7. Horizontal and vertical bending waves on a beam with mass supports: (a) attenuation spectrum; (b) Bloch wave number spectrum.

wavelength (from $\lambda_{By} = 2\pi/k_{By}$, where k_{By} is given by equation (2.26d)) coincides with the repeat length ℓ . They occur at 1181, 3604, 6298 Hz, etc. The unequal spacing of the pinned–pinned frequencies is due to the fact that bending waves have a non-linear relationship between the free wave number and frequency.

4.2.4. Horizontal and vertical bending waves

The Bloch propagation constant γ was calculated from equation (3.27), and the attenuation and Bloch wave number are shown in Figures 7(a) and 7(b) respectively. Two of

the four curves are identical to the curves in Figure 6, these represent vertical bending waves. The other two curves represent horizontal bending waves. Horizontal and vertical bending waves are uncoupled (see section 3.2.4), and so the corresponding Bloch waves travel independently. The pinned–pinned frequencies of vertical bending waves are 1181, 3604 and 6298 Hz, as in section 4.2.3, and they coincide with the upper bounds of the second, fourth and sixth stopping bands. The first, third and fifth stopping bands have upper bounds of 549, 2032, 4094 Hz, respectively; these are the pinned–pinned frequencies of horizontal bending waves.

4.2.5. Horizontal/vertical bending and torsional waves

The Bloch propagation constant γ was calculated from equation (3.30), assuming that the support points were positioned off-centre at $x' = h_x/2$ and $y' = -h_y/2$. The spectra of attenuation and Bloch wave number are shown in Figures 8(a) and 8(b) respectively. There are five solutions. Two of them are nearfield solutions; the other three solutions show passing/stopping band behaviour. In some frequency intervals, two of these three solution curves coincide, and this is indicated in Figure 8(a) by an increased line thickness. The attenuation is zero or positive in such intervals. In both cases, wave propagation takes place, as indicated by the corresponding Bloch wave number, which is between 0 and π/ℓ . Frequency intervals of propagation and zero attenuation are clearly passing bands. Frequency intervals of propagation and positive attenuation are neither passing nor stopping bands, but a halfway house, called amber bands. Amber bands have been found by other researchers, e.g., by Rebillard and Guyader [19], who studied wave coupling in periodic systems. Where amber bands occur, there is strong coupling between different wave types.

The common feature of all the spectra for mass supports is that at low frequencies, there is a passing band. Higher frequencies are increasingly dominated by stopping bands.

4.3. NUMERICAL RESULTS FOR SPRING SUPPORTS

Now a beam is considered which is supported by springs instead of masses. The springs have zero loss factor. Figures 9–13 show the attenuation spectra for the combinations of

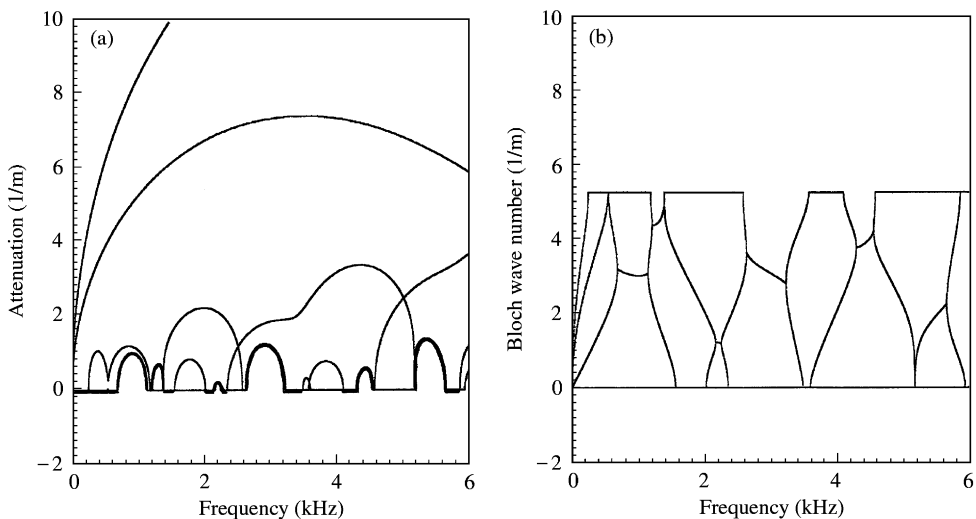


Figure 8. Horizontal/vertical bending and torsional waves on a beam with mass supports: (a) attenuation spectrum; (b) Bloch wave number spectrum.

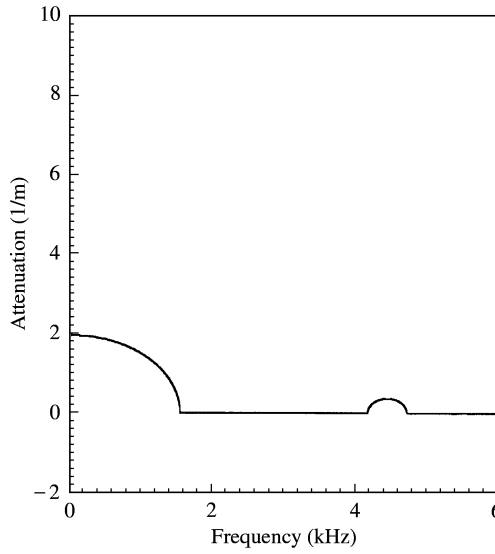


Figure 9. Attenuation spectrum of a compressional wave on a beam with spring supports.

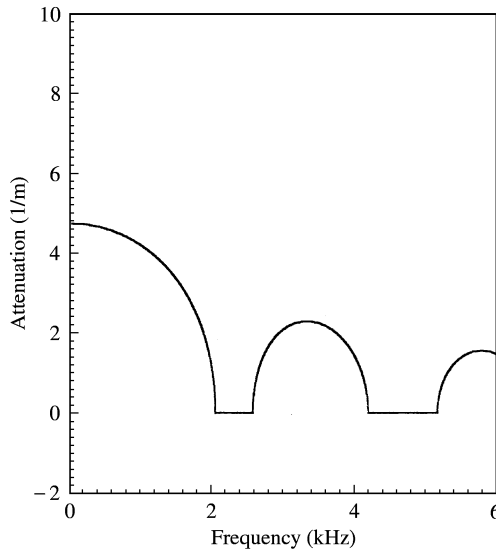


Figure 10. Attenuation spectrum of a torsional wave on a beam with spring supports.

wave types discussed in sections 4.2.1–4.2.5. Again, the spectra show alternating stopping and passing bands. The pinned–pinned frequencies are given by the same values as in the corresponding sections 4.2.1–4.2.5. Amber bands are found in Figure 13; they can be recognized by the increased line thickness.

A rigid beam on spring supports is a system that is (in contrast to one on mass supports) able to resonate. For the beam/spring system considered here, the resonance frequency is 1266 Hz for motion in the lateral and axial direction, and 2193 Hz for motion in the vertical direction. This leads to new features in the attenuation spectra. The spectra for the spring

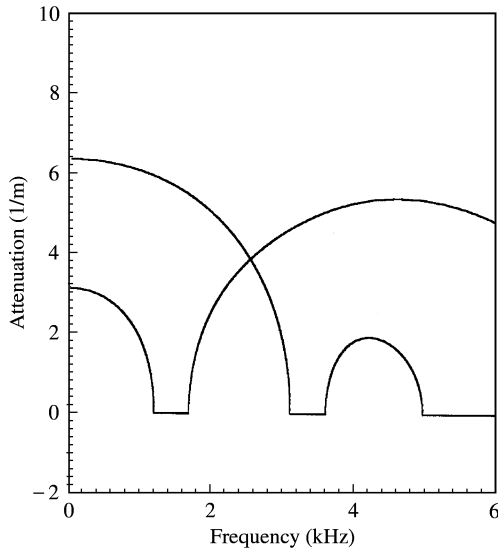


Figure 11. Attenuation spectrum of a vertical bending wave on a beam with spring supports.

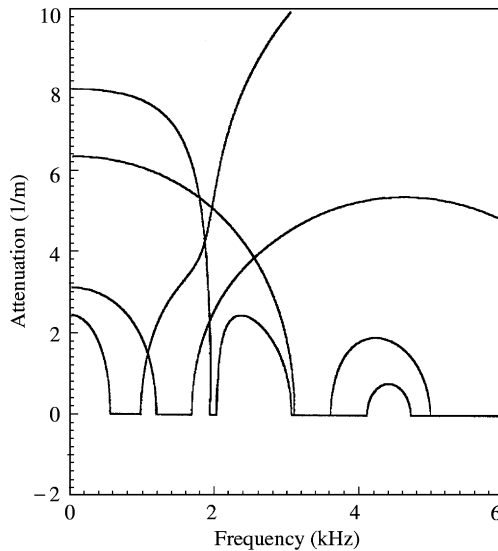


Figure 12. Attenuation spectrum of horizontal and vertical bending waves on a beam with spring supports.

supports contrast with those for the mass supports in the following ways: below the beam/spring resonance, the pinned-pinned frequencies coincide with the lower bounds of the passing bands, and above that resonance, they coincide with the upper bounds of the passing bands; the two nearfield solution curves associated with bending waves are no longer clearly separated from the curves that show passing/stopping band behaviour (compare Figures 11 and 12 with Figures 6 and 7, respectively); the passing band size increases, rather than decreases, with increasing frequency, making it easier for the waves to propagate unattenuated.

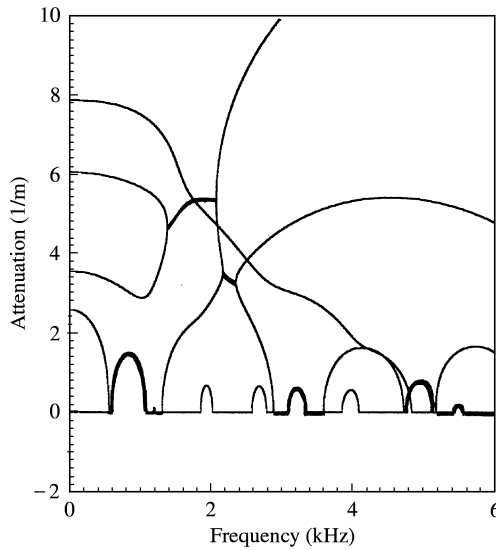


Figure 13. Attenuation spectrum of horizontal/vertical bending and torsional waves on a beam with spring supports.

Losses in the springs can be simulated by incorporating a loss factor η into the stiffnesses, i.e., by using complex stiffnesses, e.g., $s_x \rightarrow s_x (1 - i\eta)$. Such losses would lead to a positive attenuation in the passing bands. This attenuation increases with increasing loss factor.

Other supports, in particular mass/spring systems, which model the supports of a rail more realistically, have been studied. Mass/spring systems can resonate and hence act like a dynamic absorber with all the positive and negative benefits displayed by these devices. A support consisting of a single mass and spring has a single resonance frequency. Below this resonance frequency, each support behaves like a mass; the beam is then effectively mass-supported, and the attenuation spectra resemble those of section 4.2. Above this resonance frequency, each support behaves like a spring; the beam is then effectively spring-supported, and the attenuation spectra resemble those shown in Figures 9–13. Directly at this resonance frequency, each support becomes rigid (if it is undamped), and the beam is effectively simply supported.

A support consisting of several springs and/or masses, has several resonance frequencies. The support behaviour just below, just above and directly at any of these resonance frequencies is again mass-like, spring-like, and rigid respectively. At certain intermediate frequencies, the dynamic stiffness of the supports vanishes. Waves then propagate on the beam as if there were no supports at all.

5. CONCLUSIONS

A new approach based on Hamilton's principle, the superposition principle and Bloch's theorem has been applied to model the free propagation of coupled waves on a periodically supported Timoshenko beam. The beam was infinitely long and had infinitely many supports. It could carry compressional waves, torsional waves, horizontal bending waves and vertical bending waves. If a single wave type was present on the beam, its dispersion relation spectrum showed a clear passing/stopping band behaviour, with passing/stopping band pairs bounded by the pinned–pinned frequencies. If several wave types were present

on the beam, they tended to be coupled by the supports, and waves coupled in this way can behave very differently from a simple superposition of the individual wave types. The wave coupling was pronounced if the position of the support points was off the centreline of the beam. Two support types have been examined in detail: mass and spring. More complex support types, such as mass/spring systems, can be incorporated easily into the model. Predictions have been made for a supported beam that represents a rail of a typical European railway track.

ACKNOWLEDGMENTS

Part of this study (in particular sections 2.1–2.3) was supported by the ORE (now ERRI) committee C 163.

REFERENCES

1. M. J. MUNJAL and M. HECKL 1982 *Journal of Sound and Vibration* **81**, 491–500. Vibrations of a periodic rail– sleeper system excited by an oscillating stationary transverse force.
2. U. J. KURZE 1997 *ACUSTICA—Acta Acustica* **83**, 506–515. Refined calculations or improved understanding of rail vibrations?
3. A. NORDBOG 1998 *ACUSTICA—Acta Acustica* **84**, 280–288. Vertical rail vibrations: point force excitation.
4. J.-F. HAMET 1999 *ACUSTICA—Acta Acustica* **85**, 54–62. Railway noise: use of the Timoshenko model in rail vibration studies.
5. D. J. MEAD and S. MARKUS 1983 *Journal of Sound and Vibration* **90**, 1–24. Coupled flexural–longitudinal wave motion in a periodic beam.
6. MARIA A. HECKL 1992 *Fortschritte der Akustik (Proceedings of the DAGA'92 Conference, Berlin 1992)*, 1033–1036. Excitation of coupled waves on a Timoshenko beam with equally-spaced supports [in German].
7. D. J. MEAD 1996 *Journal of Sound and Vibration* **190**, 495–524. Wave propagation in continuous periodic structures: research contributions from Southampton, 1964–1995.
8. D. J. MEAD 1973 *Journal of Sound and Vibration* **27**, 235–260. A general theory of harmonic wave propagation in linear periodic systems with multiple coupling.
9. D. J. MEAD 1975 *Journal of Sound and Vibration* **40**, 19–39. Wave propagation and natural modes in periodic systems: II. Multi-coupled systems, with and without damping.
10. D. J. MEAD 1986 *Journal of Sound and Vibration* **104**, 9–27. A new method of analysing wave propagation in periodic structures: applications to periodic Timoshenko beams and stiffened plates.
11. B. R. MACE 1980 *Journal of Sound and Vibration* **73**, 473–486. Periodically stiffened fluid-loaded plates, I: response to convected harmonic pressure and free wave propagation.
12. B. R. MACE 1980 *Journal of Sound and Vibration* **73**, 487–504. Periodically stiffened fluid-loaded plates, II: response to line and point forces.
13. MARIA A. HECKL 1991 *Report to the ORE (now ERRI) Committee C 163, Department of Mathematics, Keele University, Keele, UK*. Acoustic behaviour of a periodically supported Timoshenko beam.
14. P. M. MORSE and H. FESHBACH 1953 *Methods of Theoretical Physics*. New York: McGraw-Hill Publishing Company.
15. L. CREMER and M. HECKL 1996 *Körperschall*. Berlin: Springer-Verlag; second edition.
16. MARIA A. HECKL 1995 *Acustica* **81**, 559–564. Railway noise—can random sleeper spacings help?
17. L. BRILLOUIN 1946 *Wave Propagation in Periodic Structures*. New York: McGraw-Hill Publishing Company.
18. M. ABRAMOWITZ and I. A. STEGUN 1970 *Handbook of Mathematical Functions*. New York: Dover Publications.
19. E. REBILLARD and J. L. GUYADER 1997 *Journal of Sound and Vibration* **205**, 337–354. Vibrational behaviour of lattices of plates: basic behaviour and hypersensitivity phenomena.

APPENDIX A: INTEGRAL CALCULATION

The aim is to calculate the integral

$$J = \frac{1}{2\pi} \int_{-\infty}^{\infty} \frac{f(k_z) e^{ik_z(z-z')}}{(k_z^2 - k_{Bx}^2)(k_z^2 + k_{Nx}^2)} dk_z, \tag{A1}$$

which appears in equation (2.31) of the main text. $f(k_z)$ is either a symmetrical or an antisymmetrical function of k_z .

The singularities in the integrand (see Figure A1) suggest using the calculus of residues to determine the integral in equation (A1). This involves integration along a closed contour in the complex k_z -plane.

Case 1: $z - z' < 0$

The integration contour chosen for this case is shown in Figure A2(a). The path along the real k_z -axis is closed by a semicircle in the lower half-plane with a radius tending towards infinity. The contribution to the integral along the semicircle vanishes, because $z - z' < 0$. The contour encloses the singularities at $-k_{Bx}$ and $-ik_{Nx}$. The residues of the integrand at these points are

$$\begin{aligned} \text{Res}(-k_{Bx}) &= \frac{1}{2\pi} \frac{f(-k_{Bx}) e^{-ik_{Bx}(z-z')}}{-2k_{Bx}(k_{Bx}^2 + k_{Nx}^2)}, \\ \text{Res}(-ik_{Nx}) &= \frac{1}{2\pi} \frac{f(-ik_{Nx}) e^{k_{Nx}(z-z')}}{2ik_{Nx}(k_{Bx}^2 + k_{Nx}^2)}. \end{aligned}$$

The value of the integral J can then be written as

$$\begin{aligned} J &= -2\pi i [\text{Res}(-k_{Bx}) + \text{Res}(-ik_{Nx})] \\ &= \frac{i}{2(k_{Bx}^2 + k_{Nx}^2)} \left[\frac{f(-k_{Bx}) e^{-ik_{Bx}(z-z')}}{k_{Bx}} - \frac{f(-ik_{Nx}) e^{k_{Nx}(z-z')}}{ik_{Nx}} \right]. \end{aligned} \tag{A2}$$

The minus sign in front of the term $2\pi i$ is due to the fact that the integration contour is followed in the clockwise direction. The inclusion of the singularity $-k_{Bx}$, rather than k_{Bx} , in the integration contour has led to a result representing waves travelling away from, rather than towards, the excitation point. This is desirable from a physical point of view.

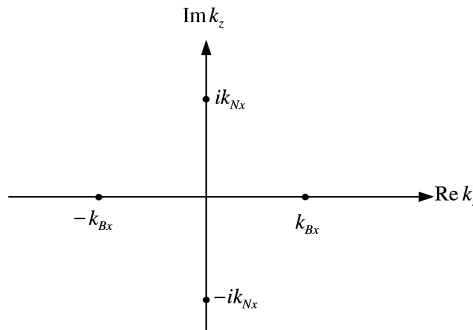


Figure A1. Position of the singularities in the complex k_z -plane.

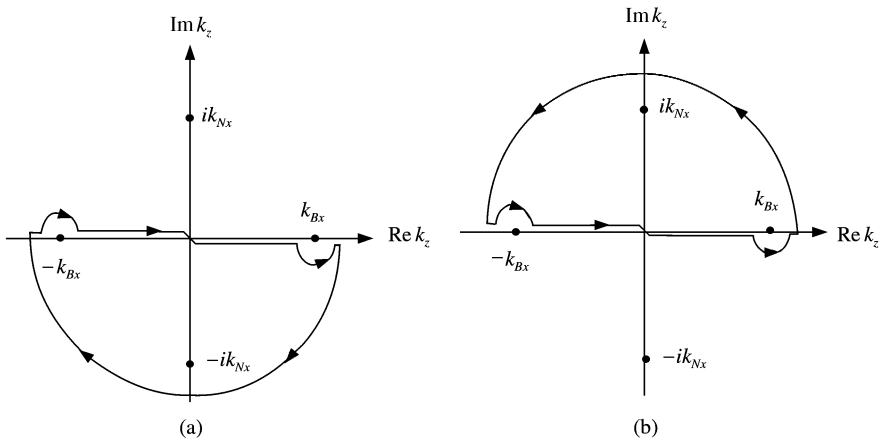


Figure A2. Integration in the complex k_z -plane: (a) for $z - z' < 0$; (b) for $z - z' \geq 0$.

Case 2: $z - z' \geq 0$

The integration contour along the real k_z -axis is again closed by a semicircle (see Figure A2(b)), but for the case $z - z' \geq 0$, the upper half-plane is chosen to make sure that there is no contribution to the integral along the semicircle. The contour encloses the singularities at k_{Bx} and ik_{Nx} , and the residues at these points are

$$Res(k_{Bx}) = \frac{1}{2\pi} \frac{f(k_{Bx})e^{ik_{Bx}(z-z')}}{2k_{Bx}(k_{Bx}^2 + k_{Nx}^2)},$$

$$Res(ik_{Nx}) = \frac{1}{2\pi} \frac{f(ik_{Nx})e^{-k_{Nx}(z-z')}}{-2ik_{Nx}(k_{Bx}^2 + k_{Nx}^2)}.$$

Taking into account the anti-clockwise direction of integration, one can write the integral J as

$$J = 2\pi i [Res(k_{Bx}) + Res(ik_{Nx})]$$

$$= \frac{i}{2(k_{Bx}^2 + k_{Nx}^2)} \left[\frac{f(k_{Bx})e^{ik_{Bx}(z-z')}}{k_{Bx}} - \frac{f(ik_{Nx})e^{-k_{Nx}(z-z')}}{ik_{Nx}} \right]. \tag{A3}$$

The propagating wave is represented by a term describing propagation in the positive z direction, i.e., away from the excitation point.

The final result, which includes both cases, $z - z' < 0$ and ≥ 0 , can be written as a summary of equations (A2) and (A3). For symmetric functions with $f(k_z) = f(-k_z)$, one obtains

$$J = \frac{i}{2(k_{Bx}^2 + k_{Nx}^2)} \left[\frac{f(k_{Bx})e^{ik_{Bx}|z-z'|}}{k_{Bx}} - \frac{f(ik_{Nx})e^{-k_{Nx}|z-z'|}}{ik_{Nx}} \right], \tag{A4}$$

and for anti-symmetric functions with $f(k_z) = -f(-k_z)$, one obtains

$$J = \frac{i \operatorname{sgn}(z - z')}{2(k_{Bx}^2 + k_{Nx}^2)} \left[\frac{f(k_{Bx})e^{ik_{Bx}|z-z'|}}{k_{Bx}} - \frac{f(ik_{Nx})e^{-k_{Nx}|z-z'|}}{ik_{Nx}} \right]. \tag{A5}$$

APPENDIX B: POLYNOMIAL COEFFICIENTS

The following abbreviations are used:

$$c_{Bx} = \cos k_{Bx}\ell, \quad s_{Bx} = \sin k_{Bx}\ell, \tag{B1a, b}$$

$$c_{Nx} = \cosh k_{Nx}\ell, \quad s_{Nx} = \sinh k_{Nx}\ell, \tag{B2a, b}$$

$$c_{By} = \cos k_{By}\ell, \quad s_{By} = \sin k_{By}\ell, \tag{B3a, b}$$

$$c_{Ny} = \cosh k_{Ny}\ell, \quad s_{Ny} = \sinh k_{Ny}\ell, \tag{B4a, b}$$

$$c_T = \cos k_T\ell, \quad s_T = \sin k_T\ell. \tag{B5a, b}$$

The polynomial in equation (3.30) has been obtained by dividing the sixth-degree polynomial

$$\cosh^6 \gamma\ell + a_6 \cosh^5 \gamma\ell + b_6 \cosh^4 \gamma\ell + c_6 \cosh^3 \gamma\ell + d_6 \cosh^2 \gamma\ell + e_6 \cosh \gamma\ell + f_6 = 0, \tag{B6}$$

by $(\cosh \gamma\ell - c_T)$. Hence the coefficients a_5, b_5, c_5, d_5 and e_5 are given by

$$a_5 = a_6 + c_T, \tag{B7}$$

$$b_5 = b_6 + a_6 c_T + c_T^2, \tag{B8}$$

$$c_5 = c_6 + b_6 c_T + a_6 c_T^2 + c_T^3, \tag{B9}$$

$$d_5 = d_6 + c_6 c_T + b_6 c_T^2 + a_6 c_T^3 + c_T^4, \tag{B10}$$

$$e_5 = e_6 + d_6 c_T + c_6 c_T^2 + b_6 c_T^3 + a_6 c_T^4 + c_T^5, \tag{B11}$$

where

$$a_6 = -c_{Bx} - c_{Nx} - c_{By} - c_{Ny} - 2c_T + iZ_x g_{Bxx} s_{Bx} - Z_x g_{Nxx} s_{Nx} + i(Z_x g_{Txx} + Z_y g_{Tyy}) s_T + iZ_y g_{Byy} s_{By} - Z_y g_{Nyy} s_{Ny}, \tag{B12}$$

$$\begin{aligned} b_6 = & c_{Bx} c_{Nx} + c_{Bx} c_{By} + c_{Bx} c_{Ny} + 2c_{Bx} c_T + c_{Nx} c_{By} + c_{Nx} c_{Ny} + 2c_{Nx} c_T + c_{By} c_{Ny} \\ & + 2c_{By} c_T + 2c_{Ny} c_T + c_T^2 \\ & - iZ_x g_{Bxx} s_{Bx} (c_{Nx} + c_{By} + c_{Ny} + 2c_T) + Z_x g_{Nxx} s_{Nx} (c_{Bx} + c_{By} + c_{Ny} + 2c_T) \\ & - i(Z_x g_{Txx} + Z_y g_{Tyy}) s_T (c_{Bx} + c_{Nx} + c_{By} + c_{Ny} + c_T) \\ & - iZ_y g_{Byy} s_{By} (c_{Bx} + c_{Nx} + c_{Ny} + 2c_T) + Z_y g_{Nyy} s_{Ny} (c_{Bx} + c_{Nx} + c_{By} + 2c_T) \\ & + Z_x Z_y \{ -g_{Bxx} g_{Byy} s_{Bx} s_{By} + g_{Nxx} g_{Nyy} s_{Nx} s_{Ny} + (-g_{Txx} g_{Tyy} + g_{Txy} g_{Tyx}) s_T^2 \\ & - i g_{Bxx} g_{Nyy} s_{Bx} s_{Ny} - i g_{Nxx} g_{Byy} s_{Nx} s_{By} \\ & - g_{Txx} g_{Byy} s_{By} s_T - i g_{Txx} g_{Nyy} s_{Ny} s_T - g_{Tyy} g_{Bxx} s_{Bx} s_T - i g_{Tyy} g_{Nxx} s_{Nx} s_T \}, \tag{B13} \end{aligned}$$

$$\begin{aligned}
c_6 = & -c_{Bx}c_{Nx}c_{By} - c_{Bx}c_{Nx}c_{Ny} - 2c_{Bx}c_{Nx}c_T - c_{Bx}c_{By}c_{Ny} - 2c_{Bx}c_{By}c_T - 2c_{Bx}c_{Ny}c_T \\
& - c_{Bx}c_T^2 - c_{Nx}c_{By}c_{Ny} - 2c_{Nx}c_{Ny}c_T - 2c_{Nx}c_{By}c_T - c_{Nx}c_T^2 - c_{By}c_T^2 - 2c_{By}c_{Ny}c_T - c_{Ny}c_T^2 \\
& - iZ_x g_{Bxx} s_{Bx} (-c_{Nx}c_{Ny} - c_{By}c_{Ny} - 2c_{Ny}c_T - c_{Nx}c_{By} - 2c_{Nx}c_T - 2c_{By}c_T - c_T^2) \\
& + Z_x g_{Nxx} s_{Nx} (-c_{Bx}c_{Ny} - c_{Bx}c_{By} - 2c_{Bx}c_T - c_{By}c_{Ny} - 2c_{Ny}c_T - 2c_{By}c_T - c_T^2) \\
& + (Z_x g_{Txx} + Z_y g_{Tyy}) i s_T (c_{Bx}c_{Nx} + c_{Bx}c_{By} + c_{Bx}c_{Ny} + c_{Bx}c_T \\
& + c_{Nx}c_{By} + c_{Nx}c_{Ny} + c_{Nx}c_T + c_{By}c_{Ny} + c_{By}c_T + c_{Ny}c_T) \\
& + iZ_y g_{Byy} s_{By} (c_{Bx}c_{Nx} + c_{Bx}c_{Ny} + 2c_{Bx}c_T + c_{Nx}c_{Ny} + 2c_{Nx}c_T + 2c_{Ny}c_T + c_T^2) \\
& + Z_y g_{Nyy} s_{Ny} (-c_{Bx}c_{Nx} - c_{Bx}c_{By} - 2c_{Bx}c_T - c_{Nx}c_{By} - 2c_{Nx}c_T - 2c_{By}c_T - c_T^2) \\
& + Z_x Z_y \{ g_{Bxx} g_{Byy} s_{Bx} s_{By} (c_{Nx} + c_{Ny} - 2c_T) + g_{Nxx} g_{Nyy} s_{Nx} s_{Ny} (-c_{Bx} - c_{By} - 2c_T) \\
& + (-g_{Txx} g_{Tyy} + g_{Txy} g_{Tyx}) s_T^2 (-c_{Bx} - c_{Nx} - c_{By} - c_{Ny}) \\
& + i g_{Bxx} g_{Nyy} s_{Bx} s_{Ny} (c_{Nx} + c_{By} + 2c_T) + i g_{Nxx} g_{Byy} s_{Nx} s_{By} (c_{Bx} + c_{Ny} + 2c_T) \\
& + g_{Txx} g_{Byy} s_{By} s_T (c_{Bx} + c_{Nx} + c_{Ny} + c_T) \\
& + i g_{Txx} g_{Nyy} s_{Ny} s_T (c_{Bx} + c_{Nx} + c_{By} + c_T) \\
& + g_{Tyy} g_{Bxx} s_{Bx} s_T (c_{Nx} + c_{By} + c_{Ny} + c_T) \\
& + i g_{Tyy} g_{Nxx} s_{Nx} s_T (c_{Bx} + c_{By} + c_{Ny} + c_T) \}, \tag{B14}
\end{aligned}$$

$$\begin{aligned}
d_6 = & c_{Bx}c_{Nx}c_{By}c_{Ny} + 2c_{Bx}c_{Nx}c_{By}c_T + 2c_{Bx}c_{Nx}c_{Ny}c_T + c_{Bx}c_{Nx}c_T^2 + 2c_{Bx}c_{By}c_{Ny}c_T \\
& + c_{Bx}c_{By}c_T^2 + c_{Bx}c_{Ny}c_T^2 + 2c_{Nx}c_{By}c_{Ny}c_T + c_{Nx}c_{By}c_T^2 + c_{Nx}c_{Ny}c_T^2 + c_{By}c_{Ny}c_T^2 \\
& - iZ_x g_{Bxx} s_{Bx} (c_{Nx}c_{By}c_{Ny} + 2c_{Nx}c_{Ny}c_T + 2c_{By}c_{Ny}c_T + c_{Ny}c_T^2 + 2c_{Nx}c_{By}c_T + c_{Nx}c_T^2 + c_{By}c_T^2) \\
& + Z_x g_{Nxx} s_{Nx} (c_{Bx}c_{By}c_{Ny} + 2c_{Bx}c_{Ny}c_T + 2c_{Bx}c_{By}c_T + c_{Bx}c_T^2 + 2c_{By}c_{Ny}c_T + c_{Ny}c_T^2 + c_{By}c_T^2) \\
& - (Z_x g_{Txx} + Z_y g_{Tyy}) i s_T (c_{Bx}c_{Nx}c_{By} + c_{Bx}c_{Nx}c_{Ny} + c_{Bx}c_{Nx}c_T + c_{Bx}c_{Nx}c_{Ny} + c_{Bx}c_{By}c_T \\
& + c_{Bx}c_{Ny}c_T + c_{Nx}c_{By}c_{Ny} + c_{Nx}c_{By}c_T + c_{Nx}c_{Ny}c_T + c_{By}c_{Ny}c_T) \\
& - iZ_y g_{Byy} s_{By} (c_{Bx}c_{Nx}c_{Ny} + 2c_{Bx}c_{Nx}c_T + 2c_{Bx}c_{Ny}c_T + c_{Bx}c_T^2 + 2c_{Nx}c_{Ny}c_T + c_{Nx}c_T^2 + c_{Ny}c_T^2) \\
& + Z_y g_{Nyy} s_{Ny} (c_{Bx}c_{Nx}c_{By} + 2c_{Bx}c_{Nx}c_T + 2c_{Bx}c_{By}c_T + c_{Bx}c_T^2 + 2c_{Nx}c_{By}c_T + c_{Nx}c_T^2 + c_{By}c_T^2) \\
& + Z_x Z_y \{ -g_{Bxx} g_{Byy} s_{Bx} s_{By} (c_{Nx}c_{Ny} + 2c_{Nx}c_T + 2c_{Ny}c_T + c_T^2) \\
& + g_{Nxx} g_{Nyy} s_{Nx} s_{Ny} (c_{Bx}c_{By} + 2c_{Bx}c_T + 2c_{By}c_T + c_T^2) \\
& + (-g_{Txx} g_{Tyy} + g_{Txy} g_{Tyx}) s_T^2 (c_{Bx}c_{Nx} + c_{Bx}c_{By} + c_{Bx}c_{Ny} + c_{Nx}c_{By} \\
& + c_{Nx}c_{Ny} + c_{By}c_{Ny}) \\
& - i g_{Bxx} g_{Nyy} s_{Bx} s_{Ny} (c_{Nx}c_{By} + 2c_{Nx}c_T + 2c_{By}c_T + c_T^2)
\end{aligned}$$

$$\begin{aligned}
& -i g_{Nxx} g_{Byy} s_{Nx} s_{By} (c_{Bx} c_{Ny} + 2c_{Bx} c_T + 2c_{Ny} c_T + c_T^2) \\
& - g_{Txx} g_{Byy} s_{By} s_T (c_{Bx} c_{Nx} + c_{Bx} c_{Ny} + c_{Bx} c_T + c_{Nx} c_{Ny} + c_{Nx} c_T + c_{Ny} c_T) \\
& -i g_{Txx} g_{Nyy} s_{Ny} s_T (c_{Bx} c_{Nx} + c_{Bx} c_{By} + c_{Bx} c_T + c_{Nx} c_{By} + c_{Nx} c_T + c_{By} c_T) \\
& - g_{Tyy} g_{Bxx} s_{Bx} s_T (c_{Nx} c_{By} + c_{Nx} c_{Ny} + c_{Nx} c_T + c_{By} c_{Ny} + c_{By} c_T + c_{Ny} c_T) \\
& -i g_{Tyy} g_{Nxx} s_{Nx} s_T (c_{Bx} c_{By} + c_{Bx} c_{Ny} + c_{Bx} c_T + c_{By} c_{Ny} + c_{By} c_T + c_{Ny} c_T) \}, \\
\end{aligned} \tag{B15}$$

$$\begin{aligned}
e_6 = & -2c_{Bx} c_{Nx} c_{By} c_{Ny} c_T - c_{Bx} c_{Nx} c_{By} c_T^2 - c_{Bx} c_{Nx} c_{Ny} c_T^2 - c_{Bx} c_{By} c_{Ny} c_T^2 - c_{Nx} c_{By} c_{Ny} c_T^2 \\
& + i Z_x g_{Bxx} s_{Bx} (2c_{Nx} c_{By} c_{Ny} c_T + c_{Nx} c_{Ny} c_T^2 + c_{By} c_{Ny} c_T^2 + c_{Nx} c_{By} c_T^2) \\
& + Z_x g_{Nxx} s_{Nx} (-2c_{Bx} c_{By} c_{Ny} c_T - c_{Bx} c_{Ny} c_T^2 - c_{Bx} c_{By} c_T^2 - c_{By} c_{Ny} c_T^2) \\
& + i (Z_x g_{Txx} + Z_y g_{Tyy}) s_T (c_{Bx} c_{Nx} c_{By} c_{Ny} + c_{Bx} c_{Nx} c_{By} c_T + c_{Bx} c_{Nx} c_{Ny} c_T \\
& + c_{Bx} c_{By} c_{Ny} c_T + c_{Nx} c_{By} c_{Ny} c_T) \\
& + i Z_y g_{Byy} s_{By} (2c_{Bx} c_{Nx} c_{Ny} c_T + c_{Bx} c_{Nx} c_T^2 + c_{Bx} c_{Ny} c_T^2 + c_{Nx} c_{Ny} c_T^2) \\
& + Z_y g_{Nyy} s_{Ny} (-2c_{Bx} c_{Nx} c_{By} c_T - c_{Bx} c_{Nx} c_T^2 - c_{Bx} c_{By} c_T^2 - c_{Nx} c_{By} c_T^2) \\
& + Z_x Z_y \{ g_{Bxx} g_{Byy} s_{Bx} s_{By} (2c_{Nx} c_{Ny} c_T + c_{Ny} c_T^2 + c_{Nx} c_T^2) \\
& + g_{Nxx} g_{Nyy} s_{Nx} s_{Ny} (-2c_{Bx} c_{By} c_T - c_{Bx} c_T^2 - c_{By} c_T^2) \\
& + (-g_{Txx} g_{Tyy} + g_{Txy} g_{Tyx}) s_T^2 (-c_{Bx} c_{Nx} c_{By} - c_{Bx} c_{Nx} c_{Ny} \\
& - c_{Bx} c_{By} c_{Ny} - c_{Nx} c_{By} c_{Ny}) \\
& + i g_{Bxx} g_{Nyy} s_{Bx} s_{Ny} (2c_{Nx} c_{By} c_T + c_{By} c_T^2 + c_{Nx} c_T^2) \\
& + i g_{Nxx} g_{Nyy} s_{Nx} s_{By} (2c_{Bx} c_{Ny} c_T + c_{Bx} c_T^2 + c_{Ny} c_T^2) \\
& + g_{Txx} g_{Byy} s_{By} s_T (c_{Bx} c_{Nx} c_{Ny} + c_{Bx} c_{Nx} c_T + c_{Bx} c_{Ny} c_T + c_{Nx} c_{Ny} c_T) \\
& + i g_{Txx} g_{Nyy} s_{Ny} s_T (c_{Bx} c_{Nx} c_{By} + c_{Bx} c_{Nx} c_T + c_{Bx} c_{By} c_T + c_{Nx} c_{By} c_T) \\
& + g_{Tyy} g_{Bxx} s_{Bx} s_T (c_{Nx} c_{By} c_{Ny} + c_{Nx} c_{By} c_T + c_{Nx} c_{Ny} c_T + c_{By} c_{Ny} c_T) \\
& + i g_{Tyy} g_{Nyy} s_{Nx} s_T (c_{Bx} c_{By} c_{Ny} + c_{Bx} c_{By} c_T + c_{Bx} c_{Ny} c_T + c_{By} c_{Ny} c_T) \}. \\
\end{aligned} \tag{B16}$$